A reduced order model for investigating the dynamics of the Gen-IV LFR coolant pool

A reduced order model for investigating the dynamics of the Gen-IV LFR coolant pool

Stefano Lorenzi[1]
E-mail: stefano.lorenzi@polimi.it

Antonio Cammi[1]
E-mail: antonio.cammi@polimi.it

Lelio Luzzi[1,*]
E-mail: lelio.luzzi@polimi.it

Gianluigi Rozza[2]
E-mail: gianluigi.rozza@sissa.it

[1] Politecnico di Milano – Department of Energy
via la Masa 34 – 20156, Milano, Italy

[2] SISSA, International School for Advanced Studies, Mathematics Area, mathLab,
via Bonomea 265 – 34136, Trieste, Italy

Abstract

In the control field, the study of the system dynamics is usually carried out relying on lumped-parameter or one-dimensional modelling. Even if these approaches are well suited for control purposes since they provide fast-running simulations and are easy to linearize, they may not be sufficient to deeply assess the complexity of the systems, in particular where spatial phenomena have a significant impact on dynamics. Reduced Order Methods (ROM) can offer the proper trade-off between computational cost and solution accuracy. In this work, a reduced order model for the spatial description of the Gen-IV LFR coolant pool is developed for the purpose of being employed in a control-oriented plant simulator of the ALFRED reactor. The spatial modelling of the reactor pool is based on the POD-FV-ROM procedure, previously developed with the aim of extending the literature approach based on Finite Element to the Finite Volume approximation of the Navier-Stokes equations, and building a reduced order model capable of handling turbulent flows modelled through the RANS equations. The mentioned approach is employed to build a ROM-based component of the ALFRED simulator for the coolant pool. The possibility of varying the input variables of the model has been also undertaken. In particular, the lead velocity at the Steam Generator outlet has been considered as a parametrized boundary condition since it can be a possible control variable. The results have turned out to be very satisfactory in terms of both accuracy and computational time. As a major outcome of the ROM model, it has been proved that its behaviour is more accurate than a 0D-based model without requiring an excessive computational cost.

Keywords: Proper Orthogonal Decomposition, Parametrized Navier-Stokes Equation, Reduced Order Modelling, Control-oriented modelling, Lead-cooled Fast Reactor.

* Corresponding author: Politecnico di Milano, via La Masa 34, 20156 Milano, Italy. Tel.: +39 02 2399 6326.
Email address: lelio.luzzi@polimi.it (L. Luzzi).

1. Introduction

Numerical simulation of complex systems requires a substantial computational effort but it is essential in engineering applications. Even if the computational power is becoming more and more available, the need to find a trade-off between computational cost and solution accuracy is a major issue especially in the control field (Gunzburger, 2003; Rozza, et al., 2008; Lorenzi et al., 2015). In this context, the study of the system dynamics is usually performed relying on lumped-parameter models (Ogata, 2009; Levine, 2011). The overall system modelling is represented by a set of Ordinary Differential Equations (ODEs), which are suitable for control purposes since they can be easily linearized allowing the study of the system by linear analysis tools. In addition, the set of ODEs usually fulfils some requirements related to the model-based control such as fast-running simulations, a comprehensive representation of the entire plant behaviour, and the possibility to couple the plant dynamics simulator with the control system model. The adoption of such simplified descriptions precludes the possibility of exploiting all the capabilities of advanced control schemes, which can provide the control system design with spatial information regarding temperature, pressure, and mass flow rate. The adoption of models based on Partial Differential Equations (PDEs), such as the Computational Fluid Dynamics (CFD) approach for the numerical simulation of fluid flows, cannot be directly exploited for control system studies, though providing accurate dynamics simulation. Indeed, besides the high computational burden, such a modelling approach does not allow the system governing dynamics to be obtained in a direct way due to the extremely large number of degrees of freedom introduced by the discretization process.

A viable solution enabling highly detailed dynamics simulation with proper computational efficiency can be obtained by Reduced Order Methods (ROM), such as Proper Orthogonal Decomposition (POD) and Reduced Basis (RB) (Rozza et al., 2008; Hesthaven et al., 2016). The aim of a computational reduction technique is to retain the governing dynamics of a system in a rapid and reliable way (Rozza et al., 2009; Manzoni et al., 2012). The main assumption of ROM is that the behaviour of the system with respect to a parameter (physical, geometrical) or time can be represented by a small number of dominant modes. The ROM are aimed at approximating a PDE solution (or a set of ODEs) with a reduced number of degrees of freedom (Manzoni et al., 2012). ROM can be employed for instance as the basis for the synthesis and the verification of controllers (El-Farra and Christofides, 2002; Bergmann et al., 2005; Barbagallo et al., 2011) or for real-time monitoring in energy applications (Ansari et al., 2016).

In the light of the considerations described above, this work investigates the possibility of combining a high-detail modelling approach featuring spatial capabilities with the requirements demanded for a control-oriented tool based on model reduction to allow computational efficiency. To this purpose, a reduced order model for the spatial description of the coolant pool of a Lead-cooled Fast Reactor (LFR) is developed aimed at being employed in a previously realized control-oriented simulator of the reactor plant (Ponciroli et al., 2014a). This simulator, implemented with the Modelica object-oriented language (The Modelica association, 2014) in the Dymola environment (DYMOLA, 2015), currently employs a zero dimensional (0D) modelling for the dynamics description of the coolant pool of the reactor. Most of the LFRs incorporate a design with a pool-type configuration as the Advanced Lead-cooled Fast Reactor European Demonstrator (ALFRED), which is taken as reference in this work (Alemberti et al., 2014). The presence of the pool offers large thermal inertia and continuous cooling to the system ensuring higher safety margin

in case of accidents along with an enhanced compactness (Cinotti et al., 2007). Notwithstanding, several issues need to be studied such as the thermal stratification (Tenchine, 2010) and the corrosion problem, the latter possibly mitigated through a suitable oxygen control (Tucek et al., 2016). These kinds of problems cannot be thoroughly investigated by means of classic 0D/1D thermal hydraulic system codes, due to the spatial nature of the involved phenomena. On the other hand, the CFD approach is essential to capture the spatial features of the fluid flow but requires a massive computational effort.

In order to overcome these limitations, we develop a ROM model for the coolant pool of the ALFRED reactor, based on the POD technique and projection-like approach, meant to replace the 0D model currently used in the control-oriented simulator. Among several reduced order methods, POD with the snapshot technique (Sirovich, 1987; Holmes et al., 1996) is probably the most widespread in the complex fluid flow computation. POD technique was first introduced to study the coherent structures in experimental turbulent flows (Lumley, 1967; Aubry et al., 1988; Berkooz et al., 1993) but it has recently become a valuable option in the ROM framework (Cazemier et al., 1998; Weller et al., 2010; Wang et al., 2012) due to the capability of selecting the most energetic modes representing the most significant features of the system. As a first step to provide the control-oriented simulator with a ROM-based component representative of the ALFRED coolant pool, a POD-Galerkin method for Finite Volume approximation of Navier-Stokes and RANS equations (POD-FV-ROM) was previously developed (Lorenzi, 2015; Lorenzi et al., 2016). The aim of this ROM technique is both to extend the classic POD-Galerkin-ROM method (namely, POD-G-ROM, e.g., see Lassila et al., 2013; Wang et al., 2012; Iliescu and Wang, 2014) to the Finite Volume approximation of the Navier-Stokes equations and to build a reduced order model capable to handle turbulent flows modelled through the RANS equations. In this paper, the POD-FV-ROM technique has been applied to the coolant pool of the ALFRED reactor. The aim is to verify and assess the possibility of substituting some components based on zero-dimensional approach in the plant simulator with ROM-based models in order to take advantage of the high level of accuracy and the better physical description without increasing the computational burden. The coolant pool of the ALFRED reactor is meant to be a test case, although the ROM approach assessed in this work can also be valuable for various other fluid-dynamics applications in the energy field.

The paper is organized as follows. In Section 2, the ALFRED reactor and its control-oriented simulator are briefly introduced. In Section 3, a general overview on the ROM approach is presented along with the POD-FV-ROM technique. In Section 4, the mentioned POD-FV-ROM is used to build a ROM-based component of the control-oriented simulator meant to be employed for coolant pool of the ALFRED reactor. In Section 5, the simulation of some transient cases is provided in order to compare the outcomes of the zero-dimensional and the ROM-based components of the simulator for the coolant pool. Finally, some conclusions, perspectives and further developments are given in Section 6.

2. The Advanced Lead Fast Reactor European Demonstrator

2.1 Reference reactor description

The reference reactor in this work is the Advanced Lead-cooled Fast Reactor European Demonstrator (ALFRED), developed within the European FP7 LEADER Project. The Project efforts were mainly focused on the resolution of the key issues that emerged in the previous Euratom ELSY Project (Cinotti et al., 2008) to reach a new reference reactor configuration, which was used to design a fully representative scaled-down prototype. The demonstration ALFRED unit is expected to be built at ICN (Institute de Cercetari Nucleare) facility near Pitesti in southern Romania (Alemberti et al., 2013a).

ALFRED is a small-size (300 MW_{th}) pool-type LFR. The current configuration of its primary system (Alemberti et al., 2013b) is depicted in Figure 1. All the major reactor primary system components, including core, primary pumps, and Steam Generators (SGs), are contained within the reactor vessel, being located in a large lead pool inside the reactor tank. The coolant flow coming from the cold pool enters the core and, having passed through the latter, is collected in a volume (hot collector) to be distributed to eight parallel pipes and delivered to as many SGs. After leaving the SGs, the coolant enters the cold pool through the cold leg and returns to the core.

The ALFRED core is composed of wrapped hexagonal Fuel Assemblies (FAs) with pins arranged on a triangular lattice (Figure 2). The 171 FAs are subdivided into two radial zones with different plutonium fractions guaranteeing an effective power flattening, and surrounded by two rows of dummy elements (geometrically identical to the fuel assemblies but not producing thermal power) serving as a reflector. Two different and independent control rod systems have been foreseen, namely, Control Rods (CRs) and Safety Rods (SRs). Power regulation and reactivity swing compensation during the cycle are performed by the former, while the simultaneous use of both is foreseen for scram purposes, assuring the required reliability for a safe shutdown (Grasso et al., 2014). In Table 1, the main nominal parameters of ALFRED are presented.

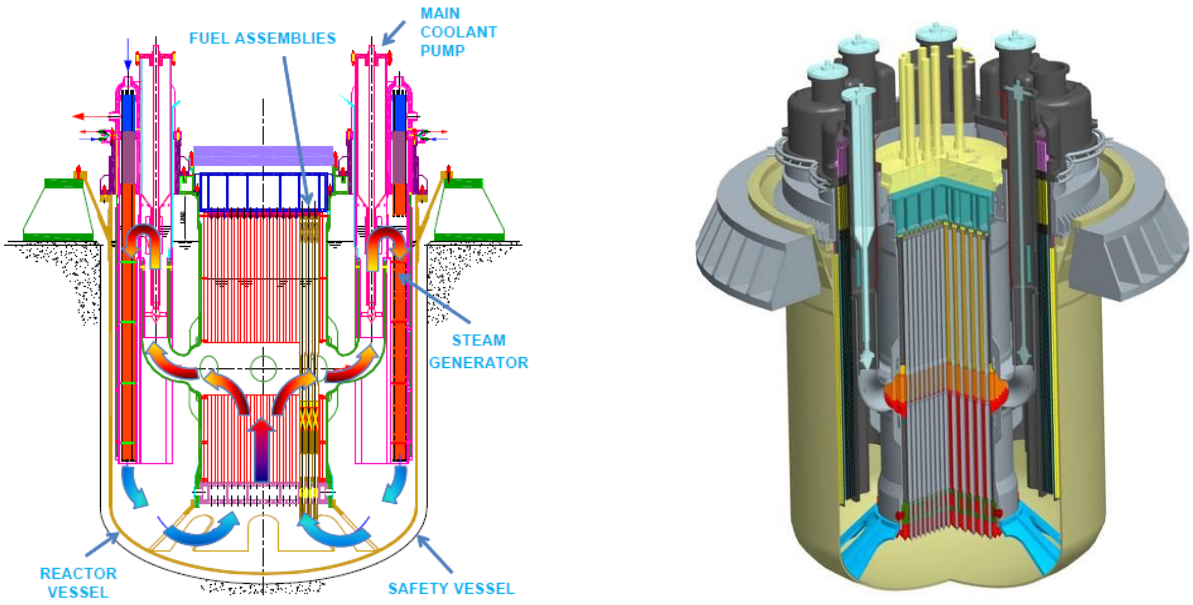

Figure 1. ALFRED nuclear power plant layout (Alemberti et al., 2013b).

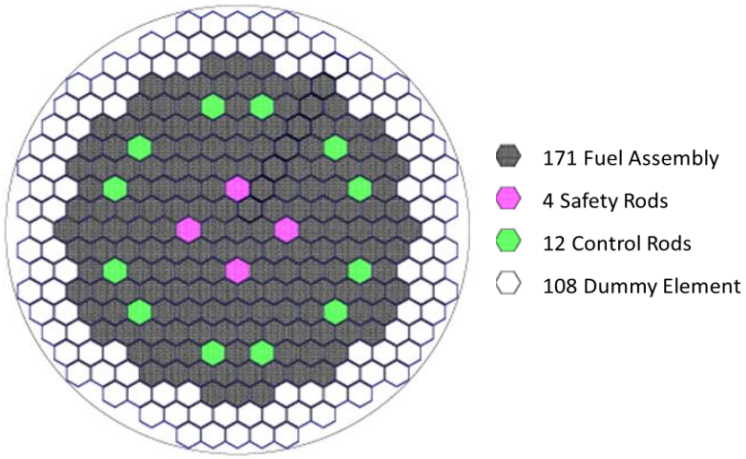

Figure 2. ALFRED core configuration (Grasso et al., 2014).

Table 1. ALFRED core parameters (Grasso et al., 2014).

Parameter	Value	Unit
Core		
Thermal power	300	MW_{th}
Coolant mass flow rate	25984	kg s^{-1}
Total number of FAs	171	-
Pins per FA	127	-
Coolant inlet temperature, T_{in}	400	°C
Coolant outlet temperature, T_{out}	480	°C
Vessel inner diameter	3.4	m
FA width	0.178	m

2.2. ALFRED control-oriented simulator

In the past years, a plant simulator of ALFRED (Ponciroli et al., 2014a) was realized in the framework of the LEADER Project by adopting the Modelica language in the Dymola software environment (DYMOLA, 2015). Modelica is a "modern, strongly typed, declarative, equation-based, and object-oriented language for modelling and simulation of complex physical system" (Fritzson, 2011). Modelica is equation-based and facilitates the system description in terms of physical/engineering principles (i.e., mass, energy, and momentum balance equations), implementing sets of Differential Algebraic Equations (DAE). The modelling approach consists of connecting different components (i.e., objects described by equations), through rigorously defined interfaces (connectors) corresponding to the physical interactions occurring with the external environment or other objects. In the ROM framework, Modelica with its component approach represents a powerful tool since it is possible to update or substitute a component with the respective ROM-based one without compromising the rest of the simulator.

Starting from the outcomes made available by the simulator and thanks to the possibility of easily linearizing the equations of the entire simulator, a decentralized control scheme was investigated based on SISO PID controller (Ponciroli et al., 2014b, Ponciroli et al., 2015a). Moreover, thanks to the simulator, a model-based assessment of the reactor start-up and the load-following capabilities of ALFRED was carried out (Ponciroli et al., 2015b, Ponciroli et al., 2016). The plant simulator (Figure 3) consists of the following essential parts: core, steam generator, primary and secondary pumps, cold and hot legs, cold pool, turbine, and condenser. The primary and secondary systems are modelled by assembling conventional components already available in a specific thermal-hydraulic

library, named *Thermopower* (Casella and Leva, 2006), and specifically developed nuclear component models, taken from the *NuKomp library* (Cammi et al., 2005). In particular, the coolant cold pool component, which is intended to be replaced by a ROM-based component, describes a free-surface lead tank on which mass and energy balances are taken (0D approach).

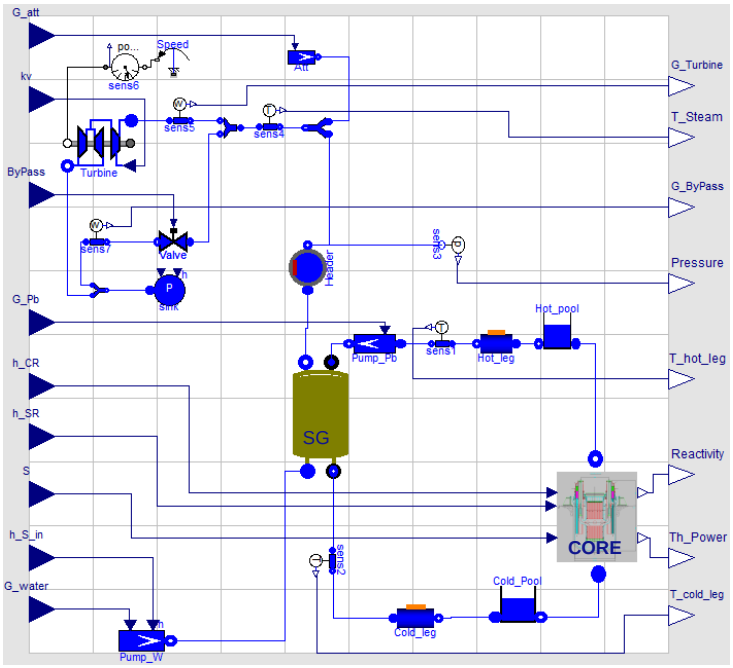

Component	Description
Core	Reactor core
Cold_pool	Pool collecting the lead coming from the SG outlet
Cold_leg	Collector between the SG outlet and the core inlet
Hot_pool	Pool collecting the lead coming from the core outlet
Hot_leg	Collector between the core outlet and the SG inlet
sens	Temperature and pressure sensor placed in the plant
Pump_Pb	Lead axial pump
SG	Steam generator
Header	Volume collecting the produced steam
Pump_W	Water pump
Turbine	Steam turbine unit
Sink	Condenser
Att	Attemperator that regulates the steam temperature

Figure 3. ALFRED plant simulator (Ponciroli et al., 2014a).

3. ROM approach

By Reduced Order Methods we mean any approach aimed at replacing a high-fidelity model, i.e., the Full Order Model (FOM), by one featuring a much lower computational complexity and retaining a comparable accuracy (Quarteroni et al., 2016; Chinesta et al., 2016).

As mentioned in the Introduction, the purpose of a computational reduction technique is to retain the governing dynamics of a system in a rapid and reliable way. In particular, reduced order methods are aimed at approximating a PDE solution (or a set of ODEs) with a reduced number of degrees of freedom. The common procedure is to solve the full order problem only for a properly selected number of instances of the input parameter (through a demanding Offline computational step), in order to be able to perform many low-cost real-time simulations (inexpensive Online computational step) for new instances of the parameter (Manzoni et al., 2012). One of the main challenges of the ROM is to find the desired compromise between the accuracy and the size of the model, i.e., the computational cost (Quarteroni et al., 2011). It is worthwhile remembering that ROMs do not replace high-fidelity discretization techniques but they are linked in a kind of algorithmic collaboration since the reduced order model is usually built upon and compared (as regards accuracy) to the FOM.

There are two main paradigms usually adopted in the reduced order methods, mainly based on projection or interpolation (Manzoni et al., 2012). To the first family belong all the *Computational Reduction Techniques* (CRT), which aim at reducing the dimension of the algebraic system through the projection onto a small subspace made by global basis functions. On the other hand, the

Surrogate Response Surfaces (SRS) family provides an approximation of the dynamics of the system by fitting a set of data obtained through numerical simulations. The main difference between the two approaches is that CRTs are problem-dependent methods whereas the SRS paradigm is problem-independent. This means that in the first approach the reduced order model is built upon physical modelling, which can be more reliable in situations far from those for which the reduced order model has been developed. In this paper, considering the control-oriented purpose applied to an innovative nuclear system for which there is no operational experience, the focus is kept on the CRT approach rather than the SRS one.

The most common CRT options are the POD and the RB methods (Rozza et al., 2008; Chinesta et al., 2015). They seek a reduced solution through a projection onto suitable low dimensional subspaces. In particular, the essential components of a CRT can be summarized as follows (Manzoni et al., 2012):

- a high-fidelity discretization technique aimed at calculating some high-fidelity PDE solutions (called snapshots) which are needed to build the reduced basis. This is usually performed employing a simulation of the FOM.
- a (Galerkin) projection. The reduced solution is usually expressed as a linear combination of basis functions. The coefficients of this combination are calculated by means of Galerkin-like projection of the equations onto the reduced space.
- offline/online computational procedures. The expensive computation of snapshots and the basis calculation can be performed just once (offline phase) and totally decoupled from the fast-running ROM simulation (online phase).
- an error estimation procedure both to assess the accuracy of the ROM and to construct a reliable, certified, and suitably reduced basis[1].

3.1. The POD-FV-ROM for RANS equations with eddy viscosity turbulent modelling

This section summarizes the POD-FV-ROM technique for RANS equations with eddy viscosity turbulent modelling (further details can be found in (Lorenzi, 2015; Lorenzi et al., 2016)). This technique is employed for the development of the reduced order model for the spatial description of the ALFRED coolant pool. The need to develop such a technique lies in the fact that the most widespread approximation scheme used in combination with the ROM techniques is the Finite Element (FE) method. On the other hand, the fluid-dynamics approach consolidated in the industrial field, and especially in nuclear engineering, is usually based on the Finite Volume approximation of the Navier-Stokes Equations (NSEs). In particular, the FV method is considered (a) robust, (b) computationally inexpensive, and (c) suitable when the conservation of the numerical flux is a relevant issue, as in the fluid-dynamics application (Eymard et al., 2000). Even if the FE can be more accurate, the FV is usually chosen for industrial applications since it is easily applicable to realistic and physical context, it does not require any particular functional framework or stabilization for flow characterized by high Reynolds number as FE, and it preserves locally the conservation laws (Versteeg and Malalasekera, 2007; Fletcher, 1996).

[1] The development of an error estimation procedure is out of the scope of this paper. Some examples can be found in (Rozza et al., 2008; Quarteroni et al., 2011; Hesthaven, 2016; Quarteroni et al., 2016).

In addition, the majority of the industrial nuclear applications deal with turbulent flows which can be modelled with several levels of accuracy according to the resolution needed for the purpose (Versteeg and Malalasekera, 2007). Although Large Eddy Simulation (LES) and Direct Numerical Simulation (DNS) are very accurate (but computationally expensive), for most engineering applications the RANS equations are sufficient to describe the main time-averaged properties of the flow (velocity, pressures, stresses, …). To this end, suitable turbulence models, such as the eddy viscosity models, can be used (e.g., Spalart-Allmaras, k–ε, k–ω) (Pope, 2000; Versteeg and Malalasekera, 2007). Employing the RANS equations allows preserving the typical industrial modelling approach when applying ROM. In this way, the use of the ROM can be achieved without modifying the codes and solvers usually adopted for industrial problems.

In the following, the POD-FV-ROM technique for RANS equations with eddy viscosity turbulent modelling is summarized. For additional information, the reader may refer to (Lassila et al., 2013; Wang et al., 2012; Kunisch and Volkwein, 2003; Iliescu and Wang, 2014) for the classic POD-G-ROM methodology, to (Sirovich, 1987; Holmes et al., 1996) for the basis of the POD theory, and to (Aubry et al., 1988; Bergmann et al., 2009; Wang et al., 2011; Balajewicz and Dowell, 2012; Balajewicz et al., 2013; Cordier et al., 2013; San and Iliescu, 2013; Osth et al., 2014; Protas et al., 2015) for the POD-ROM models with high Reynolds number based on LES and DNS simulations.

If we consider a general incompressible RANS eddy viscosity model, the equations of the FOM read:

$$\begin{cases} \boldsymbol{u}_t + (\boldsymbol{u}\cdot\nabla)\boldsymbol{u} = \nabla\cdot[-p\boldsymbol{I} + (\upsilon+\upsilon_t)(\nabla\boldsymbol{u} + (\nabla\boldsymbol{u})^{\boldsymbol{T}}) - 2/3k\boldsymbol{I}] \\ \nabla\cdot\boldsymbol{u} = 0 \end{cases} \tag{1}$$

where **u** is the velocity, p is a normalized pressure[2], υ is the kinematic viscosity, and υ_t the turbulent viscosity. The equations are given in a domain Ω with proper boundary and initial conditions. The turbulent viscosity υ_t is usually a function of one ($\tilde{\upsilon}$ in Spalart-Allmaras) or two variables (k and ε/ω in the respective models) (Versteeg and Malalasekera, 2007).

The main assumption in the ROMs based on projection technique is that the approximated solution of the problem $\boldsymbol{u}_r(\boldsymbol{x},t)$ can be expressed as linear combination of spatial modes $\boldsymbol{\varphi}_i(\boldsymbol{x})$ multiplied by temporal coefficients $a_i(t)$. If we consider the velocity, this assumption reads[3]

$$\boldsymbol{u}(\boldsymbol{x},t) \approx \boldsymbol{u}_r(\boldsymbol{x},t) = \sum_{i=1}^{N_r} a_i(t)\boldsymbol{\varphi}_i(\boldsymbol{x}) \tag{2}$$

The selection of the spatial modes is one of the crucial point in the ROM approach. A correct choice of these functions leads to an efficient ROM model, reducing the online simulation time or increasing the accuracy with respect to the Full Order Model. The POD basis

$$X_{N_r}^{POD} \coloneqq span\{\boldsymbol{\varphi}_i\}_{i=1,..,N_r} \tag{3}$$

[2] p is the thermodynamic pressure divided by the fluid density.

[3] Generally, the velocity field is decomposed in an average time-independent flow and a linear combination of time-dependent fluctuations. In this work, we consider a general formulation with no base flow.

can be built starting from a set of velocity solutions sampled at different and evenly spaced times (i.e., the snapshots)

$$\boldsymbol{u}_n(\boldsymbol{x}) \coloneqq \boldsymbol{u}(\boldsymbol{x}, t_n) \qquad n = 1, \dots, N_s \tag{4}$$

The snapshots can be numerical solutions of the NSEs (typical from LES and DNS simulations or even by the RANS equations considered in this paper) or they are obtained from experimental results. The POD basis minimizes the difference between the snapshots and the projection of the snapshots onto the spatial modes in the X-norm, given the orthonormality of the modes. If the L^2-norm is chosen, the POD basis is optimal considering the energy contained in the snapshots.

$$X_{N_r}^{POD} = \arg min \frac{1}{N_s} \sum_{n=1}^{N_s} \left\| \boldsymbol{u}_n(\boldsymbol{x}) - \sum_{i=1}^{N_r} \langle \boldsymbol{u}_n(\boldsymbol{x}), \boldsymbol{\varphi}_i(\boldsymbol{x}) \rangle_{L^2} \boldsymbol{\varphi}_i(\boldsymbol{x}) \right\|_{L^2}^2, \qquad \langle \boldsymbol{\varphi}_i(\boldsymbol{x}), \boldsymbol{\varphi}_j(\boldsymbol{x}) \rangle_{L^2} = \delta_{ij} \tag{5}$$

In order to solve Eq. (5), the following eigenvalue problem is considered:

$$C\xi_i = \lambda_i \xi_i \qquad i = 1, \dots, N_s \tag{6}$$

where $C \in \mathbb{R}^{N_s \text{ x } N_s}$ is the correlation matrix whose components are calculated as follows:

$$[C]_{kl} = \frac{1}{N_r} \langle \boldsymbol{u}_k(\boldsymbol{x}), \boldsymbol{u}_l(\boldsymbol{x}) \rangle_{L^2} \tag{7}$$

The (λ_i, ξ_i) eigenvalue – eigenvector pair is used to construct the functions of the POD basis

$$\boldsymbol{\varphi}_i(\boldsymbol{x}) = \frac{1}{\sqrt{\lambda_i}} \sum_{n=1}^{N_s} \xi_{i,n} \boldsymbol{u}_n(\boldsymbol{x}) \qquad i = 1, \dots, N_r \tag{8}$$

The POD basis functions are orthogonal and they can be suitably normalized in order to obtain $\langle \boldsymbol{\varphi}_i(\boldsymbol{x}), \boldsymbol{\varphi}_j(\boldsymbol{x}) \rangle_{L^2} = \delta_{ij}$. It is worthwhile remembering that, since the eigenvalues are sorted in descending order, the first modes have the property most of the energy present in the original solutions (Berkooz et al., 1993). This is an important feature when considering the turbulence effects since the POD truncation error leaves out the higher order modes, which − according to the energy cascade theory (Richardson, 1922; Kolmogorov, 1941) − are the less energetic but the most dissipative ones. Accordingly, the truncated POD-ROM model can blow up. In literature, this issue has been fixed by introducing proper closure modelling. Among the possible solutions, the introduction of a fictitious eddy viscosity, modelling a stabilizing dissipative term, was considered in several ways (Aubry et al., 1988; Wang et al., 2011).

The procedure described so far is close to the POD-G-ROM methodology. Hereinafter, the method moves away from the classic one due to our aim of adopting the ROM approach in a FV framework, and to consider the turbulence based on RANS equations with eddy viscosity turbulent modelling. To this aim, the face flux[4], the pressure and the turbulent viscosity can be expressed as linear combination of some spatial modes:

[4] The face flux, i.e., the scalar product between the face area vector and the velocity vector, is necessary for the discretization of the convective term in the Finite Volume method.

$$F(\boldsymbol{x},t) \approx F_r(\boldsymbol{x},t) = \sum_{i=1}^{N_r} a_i(t)\psi_i(\boldsymbol{x}) \tag{9}$$

$$p(\boldsymbol{x},t) \approx p_r(\boldsymbol{x},t) = \sum_{i=1}^{N_r} a_i(t)\chi_i(\boldsymbol{x}) \tag{10}$$

$$\upsilon_t(\boldsymbol{x},t) \approx \upsilon_{t,r}(\boldsymbol{x},t) = \sum_{i=1}^{N_r} a_i(t)\phi_i(\boldsymbol{x}) \tag{11}$$

where $\psi_i(\boldsymbol{x})$, $\chi_i(\boldsymbol{x})$ and $\phi_i(\boldsymbol{x})$ are the functions of the POD spatial basis for the face flux, the pressure and the turbulent viscosity, respectively. These spatial bases are constructed considering the eigenvectors of the correlation matrix of the velocity (Eq. 6) and the snapshots of the face flux, pressure and turbulent viscosity ($F_n(\boldsymbol{x})$, $p_n(\boldsymbol{x})$ and $\upsilon_{t,n}(\boldsymbol{x})$, obtained from the full order model) as follows:

$$\psi_i(\boldsymbol{x}) = \frac{1}{\sqrt{\lambda_i}} \sum_{n=1}^{N_s} \xi_{i,n} F_n(\boldsymbol{x}) \qquad i = 1, \dots, N_r, \tag{12}$$

$$F_n(\boldsymbol{x}) \coloneqq F(\boldsymbol{x}, t_n) \qquad n = 1, \dots, N_s, \tag{13}$$

$$\chi_i(\boldsymbol{x}) = \frac{1}{\sqrt{\lambda_i}} \sum_{n=1}^{N_s} \xi_{i,n} p_n(\boldsymbol{x}) \qquad i = 1, \dots, N_r, \tag{14}$$

$$p_n(\boldsymbol{x}) \coloneqq p(\boldsymbol{x}, t_n) \qquad n = 1, \dots, N_s. \tag{15}$$

$$\phi_i(\boldsymbol{x}) = \frac{1}{\sqrt{\lambda_i}} \sum_{n=1}^{N_s} \xi_{i,n} \upsilon_{t,n}(\boldsymbol{x}) \qquad i = 1, \dots, N_r \tag{16}$$

$$\upsilon_{t,n}(\boldsymbol{x}) \coloneqq \upsilon_t(\boldsymbol{x}, t_n) \qquad n = 1, \dots, N_s \tag{17}$$

In general, "the POD will produce the key spatial ingredients, from which our models will dynamically recreate the coherent structures as time-dependent mixtures of POD modes" (Holmes et al., 1996). Accordingly, different POD-Galerkin techniques can differ in how the spatial ingredients are built. In the POD-FV-ROM approach, the choice of expanding the different variables with the same time coefficients is due to the fact that we aim at obtaining a ROM-based model composed of just one equation (i.e., the momentum equation). In particular, if we expanded the variables with different time coefficients, we would need an equation for each time coefficient evolution. On the other hand, the continuity equation is usually neglected since the POD modes are divergence-free and moreover do not involve the pressure. For the viscosity, we could use the equations for the turbulent variables (k and ω in our case) but these equations are usually quite complicated depending also on several parameters and functions. Introducing these complicated and parameter-dependent equations in the ROM-based model may reduce its efficiency. The assumption on the time coefficients relies on the fact that we are considering a global basis for velocity, face flux, pressure and turbulent viscosity (Eq. 18).

$$\begin{pmatrix} \boldsymbol{u}(\boldsymbol{x},t) \\ F(\boldsymbol{x},t) \\ p(\boldsymbol{x},t) \\ \upsilon_t(\boldsymbol{x},t) \end{pmatrix} \approx \begin{pmatrix} \boldsymbol{u_r}(\boldsymbol{x},t) \\ F_r(\boldsymbol{x},t) \\ p_r(\boldsymbol{x},t) \\ \upsilon_{t,r}(\boldsymbol{x},t) \end{pmatrix} = \sum_{i=1}^{N_r} a_i(t) \begin{pmatrix} \boldsymbol{\varphi}_i(\boldsymbol{x}) \\ \psi_i(\boldsymbol{x}) \\ \chi_i(\boldsymbol{x}) \\ \phi_i(\boldsymbol{x}) \end{pmatrix} \tag{18}$$

As for the pressure, a similar treatment was used also in (Bergmann et al., 2009), where the authors consider the same time coefficients for velocity and pressure. It should be mentioned that Bergmann et al. use both velocity and pressure contributions for the calculation of the correlation matrix. Conversely, in the present work, the correlation matrix is based just on the velocity. This is due to the fact that firstly we want to retain the physical meaning of the energetic optimality of the POD modes. Secondly, the quantity in the correlation matrix is the information that the POD basis retains in an optimal way, and by selecting only the velocity we want the POD basis to better reproduce the velocity field rather than a combination of other quantities.

The POD-FV-ROM is not affected by the energy blow-up aforementioned since, unlike the literature cases that currently employ LES and DNS simulations to generate the snapshots, a term representing an eddy (turbulent) viscosity is already introduced thanks to the adoption of a RANS eddy viscosity model as FOM.

Due to the discretization choice for the diffusive term usually employed in the FV schemes, the boundary conditions cannot be taken into account explicitly as usually happens in the FE schemes where the Green formula is applied to the divergence operator (Jasak, 1996; Wang et al., 2012). This may be of concern if control is the purpose of the ROM model. In particular, in the fluid dynamics field, the classic control variable is the velocity at the boundary (Barbagallo et al., 2009) since it could be used to control the velocity field in the domain or an output variable of interest. In this view, if the reduced order model is directed to the synthesis of controllers, it should have the possibility of varying the velocity in order to test the several control actions. To this aim, a POD penalty method enforcing the BCs is considered (Sirisup and Karniadakis, 2005) to parametrize the velocity at the BCs in the reduced order model. As in the Spectral Methods (Gottlieb and Orszag, 1977), the Dirichlet BCs are directly incorporated in the momentum equation of the NSE as constraints

$$\boldsymbol{u}_t + (\boldsymbol{u}\cdot\nabla)\boldsymbol{u} - \nabla\cdot[-p\boldsymbol{I} + (\upsilon+\upsilon_t)(\nabla\boldsymbol{u} + (\nabla\boldsymbol{u})^{\boldsymbol{T}}) - 2/3\,k\boldsymbol{I}] + \tau\Gamma(\boldsymbol{u} - \boldsymbol{u_{BC}}) = 0 \tag{19}$$

where $\mathbf{u}_{BC}$ is the Dirichlet boundary condition, τ the penalty factor, and Γ is a null function except on the boundary where the condition is imposed (Sirisup and Karniadakis, 2005). The POD-penalty method allows incorporating and handling Dirichlet boundary conditions and it has two additional significant advantages. The first one is that this procedure enforces the approximated velocity $\mathbf{u}_r$ to satisfy the BCs of the problem. This should not be taken for granted since the approximated velocity is a linear combination of spatial functions, which in general do not satisfy the Dirichlet BCs[5], except in the case of homogeneous one. The second advantage in using the POD penalty method lies in the fact that now the equation set of the model is not autonomous anymore. In this way, some wrong long-time integration behaviour and the initial condition issue are less troublesome (Sirisup and Karniadakis, 2005). As for the penalty factor, this number is usually tuned with a sensitivity analysis (Sirisup and Karniadakis, 2005; Bizon and Continillo, 2012). In general,

[5] The functions of the basis do not respect the Dirichlet BCs since they are linear combination of snapshots, (Eq. 8), which respect the BCs in turn.

if τ tends to zero, the BCs are not enforced. On the other hand, if τ tends to infinity, the ROM model becomes ill-conditioned (Sirisup and Karniadakis, 2005).

Replacing the velocity $\boldsymbol{u}$ with $\boldsymbol{u_r}$, p with p_r and υ_t with $\upsilon_{t,r}$ in the Eq. (19), employing the approximated face flux F_r in the convective term, and applying the Galerkin projection, the following POD-Galerkin ROM for Finite Volume discretization (POD-FV-ROM) is obtained:

$$\frac{da_i(t)}{dt} = \upsilon \sum_{i=1}^{N_r} B_{ji}\, a_i(t) + \upsilon \sum_{i=1}^{N_r} BT_{ji}\, a_i(t) - \sum_{k=1}^{N_r}\sum_{i=1}^{N_r} C_{jki}\, a_k(t) a_i(t) + \sum_{k=1}^{N_r}\sum_{i=1}^{N_r} CT1_{jki}\, a_k(t) a_i(t) + \sum_{k=1}^{N_r}\sum_{i=1}^{N_r} CT2_{jki}\, a_k(t) a_i(t) - \sum_{i=1}^{N_r} A_{ji}\, a_i(t) + \tau\left(\boldsymbol{u_{BC}} \cdot \boldsymbol{D}_j - \sum_{i=1}^{N_r} E_{ji}\, a_i(t)\right) \tag{20}$$

where

$$a_j(0) = \langle \boldsymbol{\varphi}_j, \boldsymbol{u}_1(\boldsymbol{x}) \rangle_{L^2} \tag{21}$$

$$A_{ji} = \langle \boldsymbol{\varphi}_j, \nabla \chi_i \rangle_{L^2}. \tag{22}$$

$$B_{ji} = \langle \boldsymbol{\varphi}_j, \Delta \boldsymbol{\varphi}_i \rangle_{L^2}, \tag{23}$$

$$BT_{ji} = \langle \boldsymbol{\varphi}_j, \nabla \cdot \left(\nabla \boldsymbol{\varphi}_i^{\boldsymbol{T}}\right) \rangle_{L^2} \tag{24}$$

$$C_{jki} = \langle \boldsymbol{\varphi}_j, \nabla \cdot (\psi_k, \boldsymbol{\varphi}_i) \rangle_{L^2}, \tag{25}$$

$$CT1_{jki} = \langle \boldsymbol{\varphi}_j, \phi_k \Delta \boldsymbol{\varphi}_i \rangle_{L^2} \tag{26}$$

$$CT2_{jki} = \langle \boldsymbol{\varphi}_j, \nabla \cdot \phi_k \left(\nabla \boldsymbol{\varphi}_i^{\boldsymbol{T}}\right) \rangle_{L^2} \tag{27}$$

$$\boldsymbol{D}_j = \langle \boldsymbol{\varphi}_j \rangle_{L^2, \partial\Omega}, \tag{28}$$

$$E_{ji} = \langle \boldsymbol{\varphi}_j, \boldsymbol{\varphi}_i \rangle_{L^2, \partial\Omega}. \tag{29}$$

Note that the $2/3k\boldsymbol{I}$ term is neglected in the ROM model since it can be incorporated in the pressure term (Pope, 2000). The dynamical system of the time-dependent coefficients for turbulence can be expressed as follows:

$$\dot{\boldsymbol{a}} = \upsilon(\boldsymbol{B} + \boldsymbol{BT})\boldsymbol{a} - \boldsymbol{a}^{\boldsymbol{T}}(\boldsymbol{C} - \boldsymbol{CT1} - \boldsymbol{CT2})\boldsymbol{a} - \boldsymbol{Aa} + \tau(\boldsymbol{u_{BC}D} - \boldsymbol{Ea}) \tag{30}$$

The procedure proposed in this work has the advantage of being as flexible as possible, and less dependent on the turbulent modelling. In particular, the technique can be applied to any model that expresses the momentum equation as Eq. (1), disregarding the specific modelling of the turbulent viscosity[6]. In addition, since in the POD-FV-ROM the diffusive term is not modified with the Green formula, the technique can be used also whether wall functions are applied or not. Indeed, problems may arise in the treatment of the wall functions if the BCs are directly incorporated in the ROM, since the wall functions of the turbulent quantities may be neither constant nor time-independent.

[6] This is due to the choice of not projecting the equations that govern the eddy viscosity behaviour as the turbulent kinetic energy (k) and the specific rate dissipation (ω) in the k–ω modelling.

4. Reduced order model of the ALFRED pool

A reduced order model of the ALFRED coolant pool (Figure 4a) has been set up according to the POD-FV-ROM procedure described in Section 3.1. In particular, a 2D geometry (Figure 4b) of the ALFRED coolant pool is adopted, for the sake of simplicity, by taking advantage of the symmetry of the core (Figure 4c), even if the technique can be easily extended to the 3D case. In the adopted configuration, just two Steam Generators (SGs) are involved. The reduced order model is aimed at being employed in the control-oriented plant simulator of the ALFRED reactor, substituting the zero-dimensional model of the cold pool.

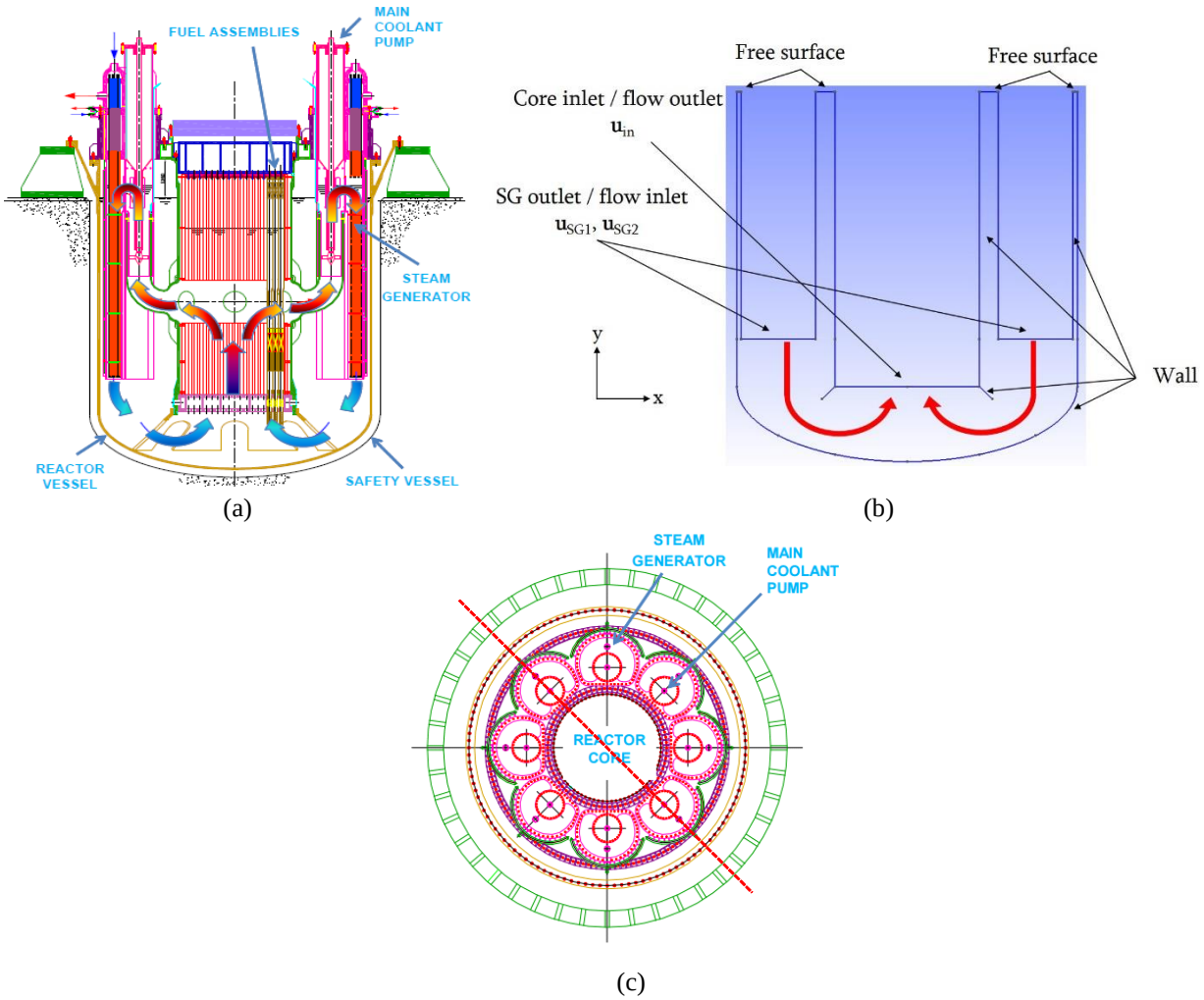

Figure 4. (a) ALFRED pool configuration (Alemberti et al., 2013b); (b) 2D geometry of the ALFRED pool model; (c) top view of the reactor (Alemberti et al., 2013b) - the red line represents the plane used for the 2D representation of the ALFRED pool).

In order to demonstrate the feasibility of employing ROM-based components in a control-oriented simulator, the possibility of varying the input variables of the model should be undertaken. In this case, the latter is represented by the fluid velocity at the SG outlet[7] ($\mathbf{u}_{SG1}$, $\mathbf{u}_{SG2}$). In particular, this could be a possible control variable employed to change the fluid velocity profile ($\mathbf{u}_{in}$) at the core inlet[8]. In addition, these variables are the connections between the cold pool component and the rest

[7] Actually, the input variable is the pump velocity, which can modify the mass flow rate inside the pool and the fluid velocity in turn. But, for the sake of simplicity, we will consider the fluid velocity at SG outlet as the control variable of the problem.

[8] The inlet temperature can be also changed whether the energy equation is considered.

of the plant, the fluid velocity at the core inlet being an input parameter for the core component since it determines the mass flow rate for each FA, and the fluid velocity at the SG outlet being an output parameter for the SG component. For this purpose, a *parametric* reduced order model of the ALFRED pool has been developed, focusing on the variation of the core inlet velocity profile following a SG outlet ($\mathbf{u}_{SG1}$, $\mathbf{u}_{SG2}$) velocity change.

4.1 The offline procedure

The offline procedure (i.e., calculation of the FOM solutions, generation of snapshots and construction of the matrix of Eq. (30)) is performed in the OpenFOAM environment (Weller et al., 1998; OpenFOAM, 2014). OpenFOAM is an open source library for numerical simulation in continuum mechanics. The toolkit is very flexible thanks to the object-oriented programming, allowing users to customise, extend and implement complex physical models. Even though the POD generation is already present in the extended version of OpenFOAM (Jasak et al., 2007), some tools have been updated or created in order to implement the offline phase of POD-FV-ROM in the library.

As a first step of the offline procedure, a CFD model (FOM model) for the ALFRED coolant pool has been developed in the OpenFOAM environment considering the boundary conditions for pressure and velocity shown in Figure 5. In particular, for the fluid velocity at the SG outlet, a range between 0.17 m/s (nominal condition) and 0.085 m/s (50% reduction with respect to the nominal condition) is spanned.

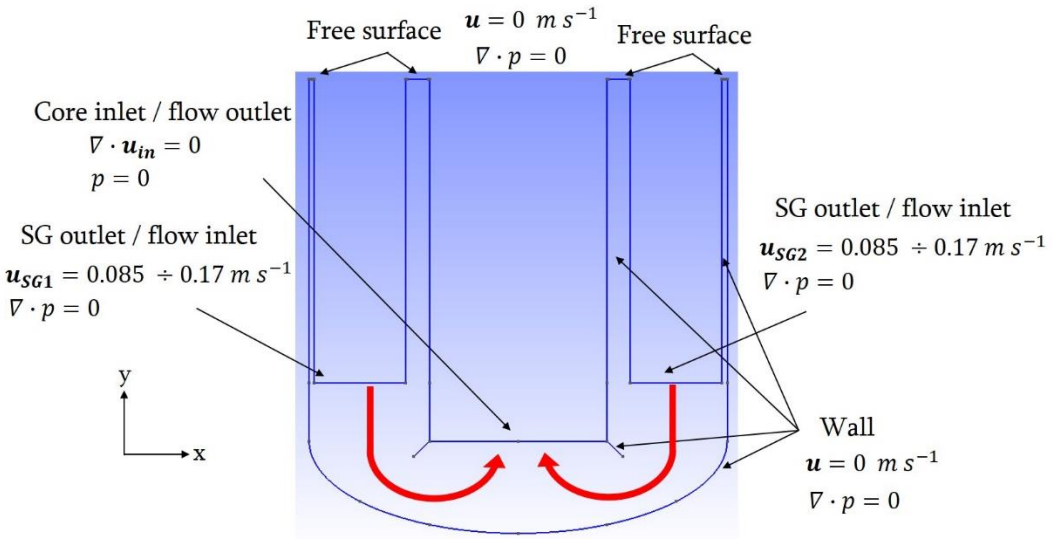

Figure 5. Boundary conditions for the ALFRED pool model.

Some numerical aspects regarding the full order model developed in OpenFOAM are pointed out in the following. As for the RANS turbulent modelling, the Shear Stress Transport (SST) formulation of the k–ω modelling (Menter, 1994; Menter et al., 2003; OpenFOAM, 2014) is selected because it is a low-Reynolds model and it blends the k–ω features near the wall and the k–ε behaviour in the bulk flow. A merged PISO-SIMPLE (PIMPLE) algorithm (Versteeg and Malalasekera, 2007; OpenFOAM, 2014) available in OpenFOAM is employed to solve the RANS in order to obtain for each time step at least a convergence of 10^{-5} for the velocity and turbulent quantities, and a convergence of 10^{-3} for the pressure. As for the numerical discretization, second-

order bounded linear schemes are employed except for the advective term of the momentum and k–ω equations, which use a second-order bounded upwind scheme and a first-order upwind scheme, respectively. A first order Euler implicit scheme is instead adopted for the time discretization. A mesh with $1.5 \cdot 10^5$ cells is adopted for a proper accuracy, and to obtain a value of y+ near unity for the application of the k–ω SST modelling without wall functions. For the sake of comparison, a steady-state comparison with respect to k–ε modelling with wall functions is performed in a nominal condition, and shows a good agreement between the outcomes of the two modelling approaches (Figure 6 and Figure 7).

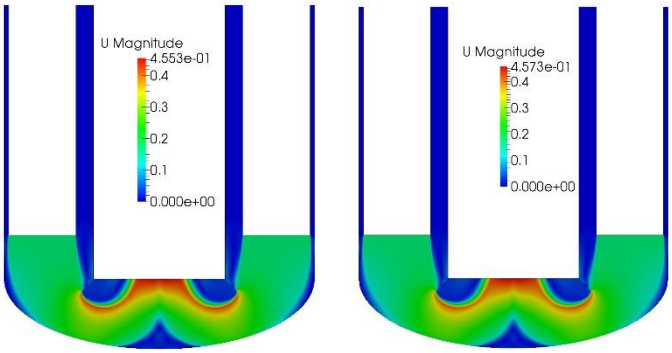

(a) (b)

Figure 6. Contours of velocity magnitude in nominal condition calculated with (a) k–ω and (b) k–ε model in the ALFRED pool.

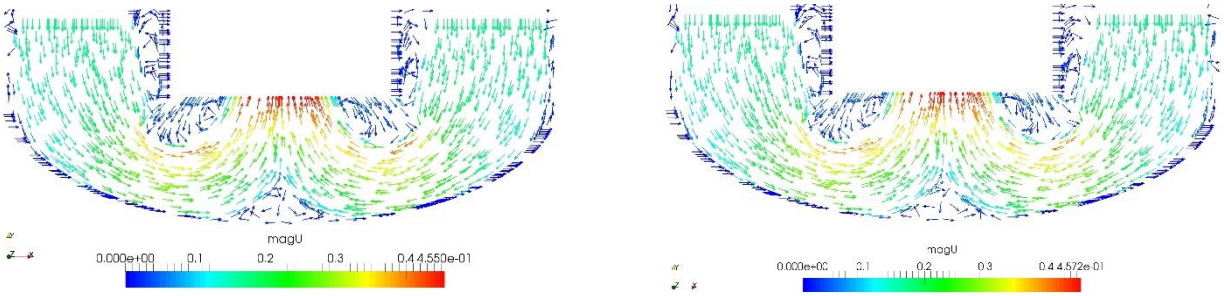

(a) (b)

Figure 7. Vectors of velocity magnitude in nominal condition calculated with (a) k–ω and (b) k–ε model in the ALFRED pool.

Sixteen transients are performed to span the range of the fluid velocity at SG outlet (i.e., the flow inlet considering the pool) between 0.17 and 0.085 m/s (Table 2). After 0.5 s, a 5 s ramp decrease of the velocity is carried out from the initial nominal value to the final value. Figure 8 represents the evolution of the contours of the velocity magnitude in Case 13, along with the profile of the velocity at the core inlet (i.e., the flow outlet considering the pool). Besides being a demanding transient both from a computational and operational point of view, it is interesting to point out the change in the velocity profile at the core inlet. After the decrease of the velocity at SG2 outlet, the profile at the core inlet is totally changed, moving from the centre of the core to the periphery. This kind of information cannot be retrieved with a zero-dimensional or 1D model, where usually the core inlet velocity is decreased to the same amount of the decrease of the SG outlet one, with an unchanged profile. Even if the field of application is control, it is clear that dealing with a model that is able to reproduce such behaviour can provide significant insights from a safety point of view. In particular, for the considered transient, the change in the core inlet profile results in the cooling modification

of different core zones, especially for the left part of the core where the velocity of the coolant is close to zero and almost no cooling action is performed.

Table 2. Transient cases performed for the construction of the parametric ROM for the ALFRED pool.

Case #	$\mathbf{u}_{SG1}$ (m/s)		$\mathbf{u}_{SG2}$ (m/s)	
	initial	final	initial	final
1	0.170	0.085	0.170	0.085
2	0.170	0.085	0.170	0.119
3	0.170	0.085	0.170	0.153
4	0.170	0.085	0.170	0.170
5	0.170	0.119	0.170	0.085
6	0.170	0.119	0.170	0.119
7	0.170	0.119	0.170	0.153
8	0.170	0.119	0.170	0.170
9	0.170	0.153	0.170	0.085
10	0.170	0.153	0.170	0.119
11	0.170	0.153	0.170	0.153
12	0.170	0.153	0.170	0.170
13	0.170	0.170	0.170	0.085
14	0.170	0.170	0.170	0.119
15	0.170	0.170	0.170	0.153
16	0.170	0.170	0.170	0.170

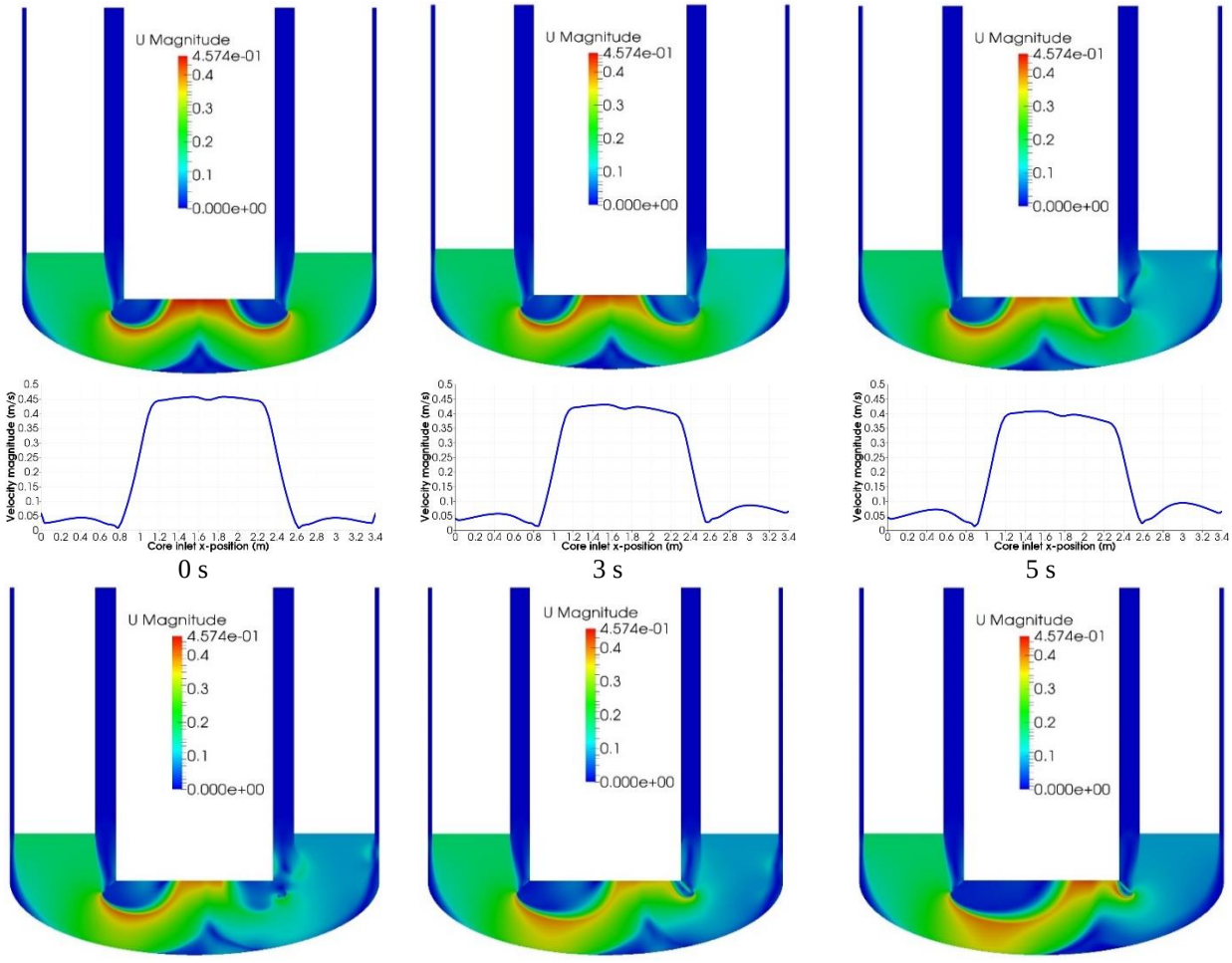

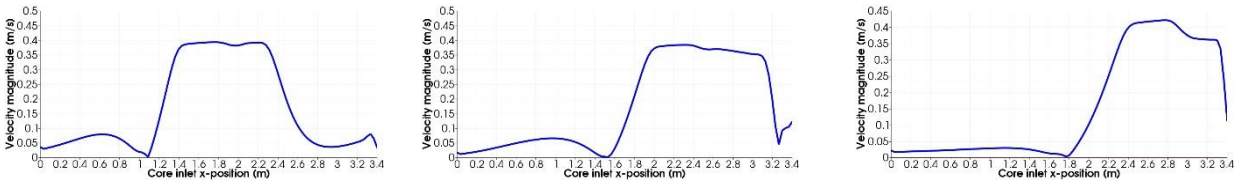

Figure 8. Evolution of the contours of the velocity magnitude in Case 13, along with the profile of the velocity magnitude at the core inlet.

4.2. The 0D model and the ROM-based component of the ALFRED pool

In the control-oriented simulator described in Section 2.2, the cold pool is modelled considering mass and energy balances (Figure 9 shows the Modelica code of the component based on the 0D approach). As pointed out in the Introduction, this kind of approach prevents the simulation tool from taking into account turbulence mixing and 3D effects, which can have a remarkable impact both on control issues (i.e., the oxygen control in LFR) and safety issues as well (e.g., as in Case 13 of the previous section, see Figure 8).

```
Model Cold_pool "Open tank with free surface"
    parameter Area A "Cross-sectional area";
    parameter Volume V0 "Volume at zero level";
    parameter Pressure pext "Surface pressure";
    parameter Length ystart "Start level"
    parameter SpecificEnthalpy hstart
    Length y(start=ystart, stateSelect=StateSelect.prefer) "Level";
    Volume V "Liquid volume";
    Mass M "Liquid mass";
    Enthalpy H "Liquid (total) enthalpy";
    Medium.SpecificEnthalpy h(start=hstart, stateSelect=StateSelect.prefer)     "Liquid specific enthalpy";
    Medium.SpecificEnthalpy hin "Inlet specific enthalpy";
    Medium.SpecificEnthalpy hout "Outlet specific enthalpy";
    Medium.AbsolutePressure p(start=pext) "Bottom pressure";
    constant Real g=Modelica.Constants.g_n;
    parameter Choices.Init.Options initOpt=Choices.Init.Options.noInit     "Initialisation option;

equation
    liquidState = Medium.setState_ph(pext, h);
    V = V0 + A*y "Liquid volume";
    M = V*Medium.density(liquidState) "Liquid mass";
    H = M*Medium.specificInternalEnergy(liquidState) "Liquid enthalpy";
    der(M) = inlet.m_flow + outlet.m_flow "Mass balance";
    der(H) = inlet.m_flow*hin + outlet.m_flow*hout "Energy balance";
    p - pext = Medium.density(liquidState)*g*y "Stevino's law";
end Cold_pool;
```

Figure 9. Modelica code of the *Cold_pool* component (Ponciroli et al., 2014a).

The *Coolant Pool ROM* component of the ALFRED reactor (Figure 10) has been developed employing the turbulent POD-FV-ROM technique summarized in Section 3.1, considering the velocity of the two SGs as parametrized boundary conditions. Accordingly, Eq. (30) is modified as follows:

$$\dot{\boldsymbol{a}} = \upsilon(\boldsymbol{B}+\boldsymbol{BT})\boldsymbol{a} - \boldsymbol{a}^{\boldsymbol{T}}(\boldsymbol{C}-\boldsymbol{CT1}-\boldsymbol{CT2})\boldsymbol{a} - \boldsymbol{Aa} + \tau(\boldsymbol{u_{SG1}D_{SG1}} + \boldsymbol{u_{SG2}D_{SG2}} - \boldsymbol{Ea}) \tag{31}$$

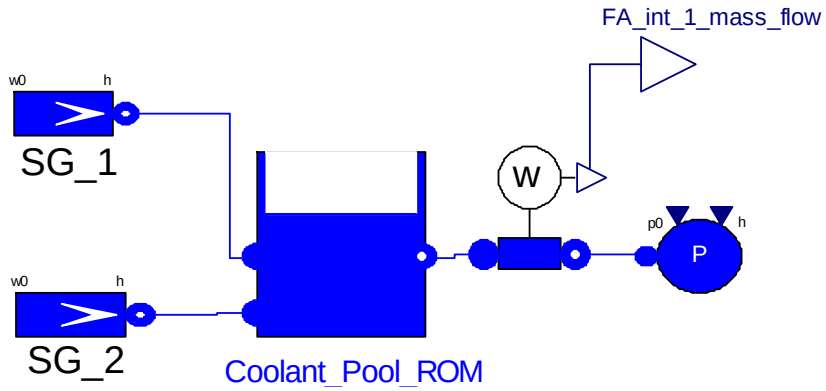

Figure 10. ROM-based component of the ALFRED pool.

Eq. (31) is implemented in the *Coolant Pool ROM* component that calculates the mass flow rate of the central FA as possible output variable (Figure 11 shows the Modelica code of the ROM-based component). In particular, the latter ($\dot{m}_{FA}$) is calculated as

$$\dot{m}_{FA} = \int \rho \, \boldsymbol{u} \cdot d\boldsymbol{A} \approx \int \rho \, \boldsymbol{u}_r \cdot d\boldsymbol{A} = \int \rho \sum_{i=1}^{N_r} a_i \boldsymbol{\varphi}_i \cdot d\boldsymbol{A} = \sum_{i=1}^{N_r} a_i \int \rho \, \boldsymbol{\varphi}_i \cdot d\boldsymbol{A} = \sum_{i=1}^{N_r} a_i \mu_i \tag{32}$$

where μ_i is the mass flow rate of central FA calculated for each function of the POD basis:

$$\mu_i = \int \rho \, \boldsymbol{\varphi}_i \cdot d\boldsymbol{A} \tag{33}$$

```
model Coolant_Pool_ROM  "ROM model for the ALFRED coolant pool";
   extends ThermoPower.Icons.Water.Tank;
   import C_function;
   parameter Integer N=79 "Number of functions in the basis";
   parameter Real nu=1.937e-7 "Kinematic viscosity";
   parameter Real A[:,:]=readMatrix("matrices.mat", "A", N,N) "A matrix of Eq. (31)";
   parameter Real B[:,:]=readMatrix("matrices.mat", "B", N,N) "B matrix of Eq. (31)";
   parameter Real BT[:,:]=readMatrix("matrices.mat", "BT", N,N) "BT matrix of Eq. (31)";
   parameter Real DSG1[:,1]=readMatrix("matrices.mat", "DSG1", N,1) "DSG1 vector of Eq. (31) - y component";
   parameter Real DSG2[:,1]=readMatrix("matrices.mat", "DSG2", N,1) "DSG2 vector of Eq. (31) - y component";
   parameter Real E[:,:]=readMatrix("matrices.mat", "E", N, N) "E matrix of Eq. (31)";
   parameter Real FA_1_flow[1,:]=readMatrix("matrices.mat", "FA_1_flow", 1,N) "μi of Eq. (33)";
   parameter Real ci[1,:]=readMatrix("matrices.mat", "ci", 1,N); "initial conditions"
   parameter Real tau=1e-2; "penalty factor"
     Real a[N,1]; "time coefficients"

equation   "Eq. 31"
  der(a)=nu*(B+BT)*a+C_function(a)-A*a+tau(inlet_SG_1.m_flow*DSG1+inlet_SG_2.m_flow*DSG2-E*a);
  FA_int_1.m_flow=-FA_1_flow[1,:]*a[:,1];

initial equation
   a=transpose(ci);
end Coolant_Pool_ROM;
```

Figure 11. Modelica code of the *Coolant pool ROM* component.

5. Simulation results

In order both to test the ROM-based component of the ALFRED coolant pool and to compare the outcomes with the zero-dimensional model, the simulation results of some transient cases are discussed in this Section. For the sake of brevity, only the results of the parametric reduced order model of the coolant pool are presented, starting from 2100 snapshots of the cases involving only the velocity variation of the second steam generator (i.e., the Cases from 13 to 16, see Table 2). To

assess the accuracy of the ROM model, the difference between the ROM and FOM model (taken as reference) is reported using the L^2 error:

$$\|e\|_{L^2} = \sqrt{\frac{\langle (\boldsymbol{u_{FOM}} - \boldsymbol{u_r}), (\boldsymbol{u_{FOM}} - \boldsymbol{u_r}) \rangle_{L^2}}{\langle \boldsymbol{u_{FOM}}, \boldsymbol{u_{FOM}} \rangle_{L^2}}} \tag{34}$$

In Figure 12, the L^2 error of the ROM model velocity is compared with 80 and 65 spatial basis functions following a velocity variation of the second SG of 10%, 30% and 50% with respect to the nominal value. For a velocity variation of 10% and 30% (i.e., $\mathbf{u}_{SG2}$ = 0.153 m/s and $\mathbf{u}_{SG2}$ = 0.119 m/s, respectively), the error is almost always lower than $1 \cdot 10^{-2}$, whereas for a velocity variation of 50% (i.e., $\mathbf{u}_{SG2}$ = 0.085 m/s) the error is between $5 \cdot 10^{-2}$ and $8 \cdot 10^{-3}$. Even if a worse performance is obtained in the latter case, the results are very promising, the maximum relative error being equal to 5%.

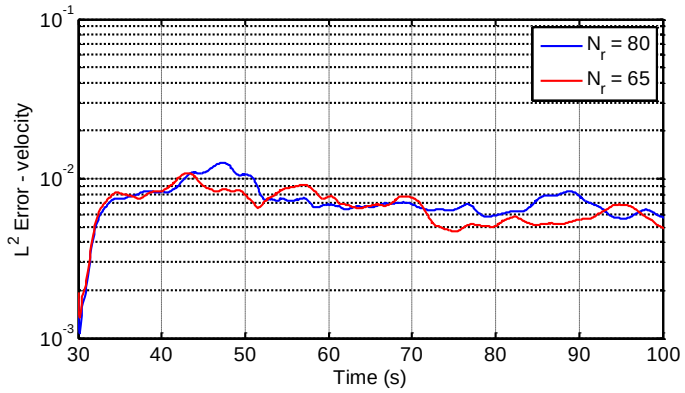

(a)

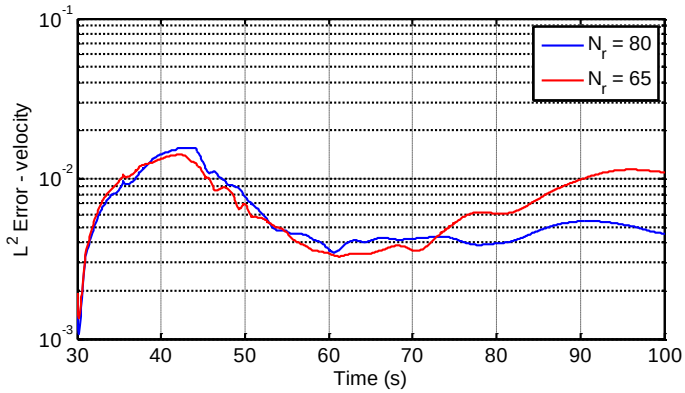

(b)

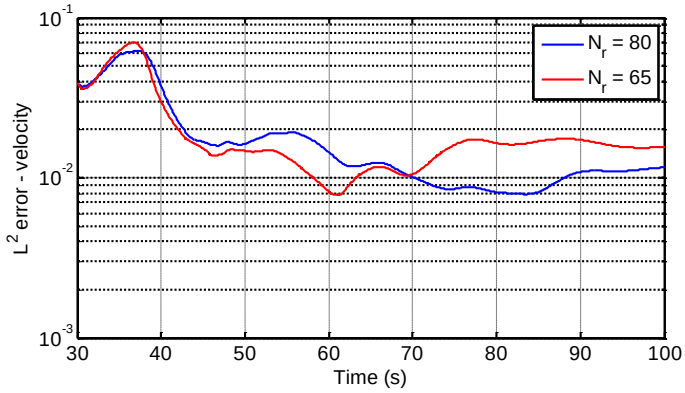

(c)

Figure 12. L^2 error of the reconstructed velocity from ROM model with N_r=80 (blue line) and N_r=65 (red line) following a velocity variation of (a) 10% - u_{SG2}=0.153 m/s; (b) 30% - u_{SG2}=0.119 m/s; (c) 50% - u_{SG2}=0.085 m/s with respect to the nominal value.

The L^2 error of the velocity field is relevant for a general assessment of the accuracy of the reduced order model. On the other hand, since the purpose is the adoption of the ROM-based component in a control-oriented simulator, the evaluation of the output variables is relevant as well. In this sense, the output variables of the coolant pool model are the inlet mass flow rates of the FA since they represent the connection between the ROM-based component of the coolant pool and the reactor core model. To this end, we consider three models of the coolant pool, namely: the FOM model, based on CFD; the developed ROM-based component; and the 0D-based component (i.e., the Cold Pool component, see Figure 9). Figure 13, Figure 14, and Figure 15 show the variation of the mass flow rate in the central FA for the three modelling approaches following a velocity variation at the outlet of the second SG of 10%, 30% and 50%, respectively.

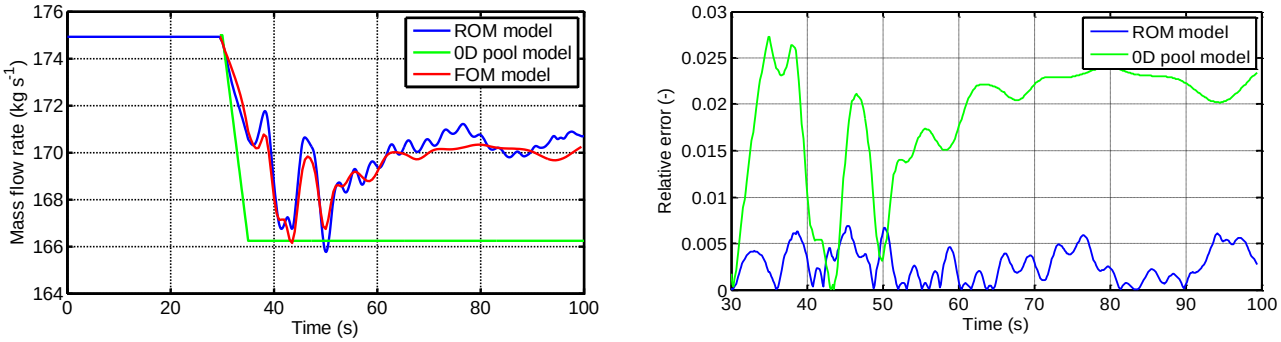

(a) (b)

Figure 13. (a) Evolution of the mass flow rate in the central FA following a velocity variation of (a) 10% - u_{SG2}=0.153 m/s with respect to the nominal value. ROM (blue line), 0D (green line) and FOM (red line) model results; (b) relative error of ROM and 0D model with respect to FOM model.

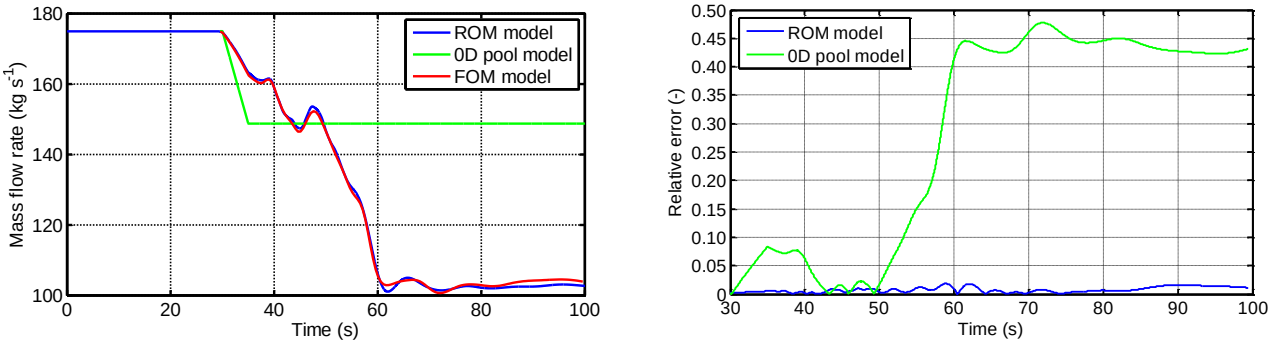

(a) (b)

Figure 14. (a) Evolution of the mass flow rate in the central FA following a velocity variation of (a) 30% - u_{SG2}=0.119 m/s with respect to the nominal value. ROM (blue line), 0D (green line) and FOM (red line) model results; (b) relative error of ROM and 0D model with respect to FOM model.

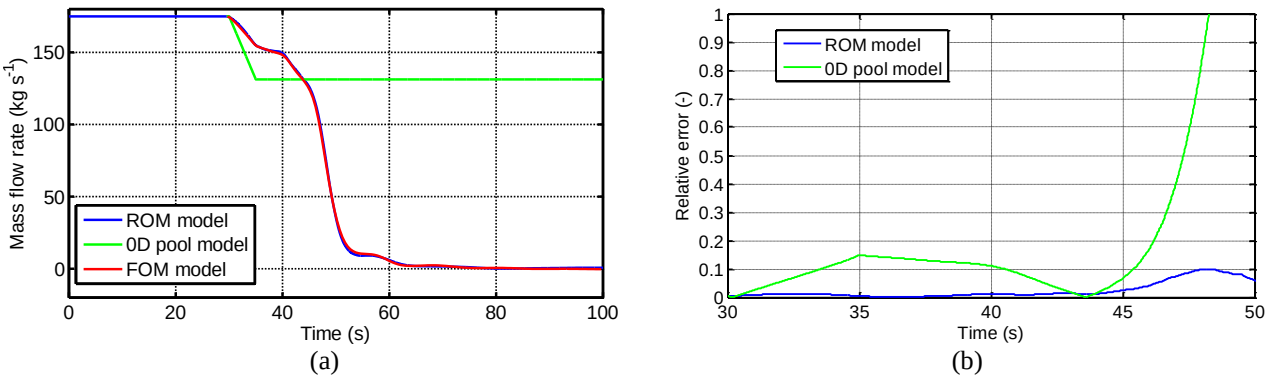

(a) (b)

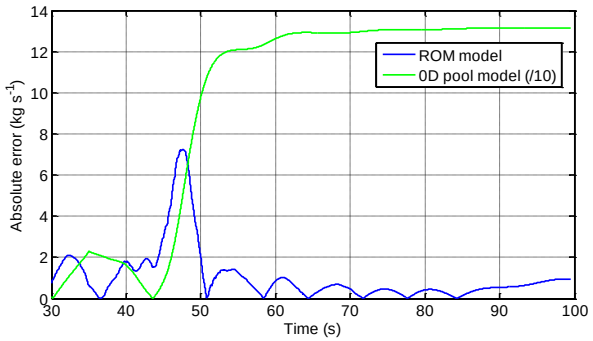

(c)

Figure 15. (a) Evolution of the mass flow rate in the central FA following a velocity variation of (a) 50% - u_{SG2}=0.085 m/s with respect to the nominal value. ROM (blue line), 0D (green line) and FOM (red line) model results; (b) relative error of ROM and 0D model with respect to FOM model (the time is limited to 50 s since the FOM mass flow rate approaches a very small value); (c) absolute error of ROM and 0D model with respect to FOM model (the value for 0D model is divided by 10 for the sake of readability).

In general, there is a good agreement between the ROM-based component (N_r=80) and the FOM. It is worthwhile emphasising that for all the three cases, the 0D model of the cold pool completely fails in reproducing the transient behaviour and the final mass flow rate value. This can be explained considering the Figure 8. In this asymmetric transient, the spatial information of the velocity is crucial since the core inlet profile moves to the periphery of the core. This effect is well represented in the full order model and in the derived reduced order model. On the other hand, the 0D model is not able to capture this spatial information and the outcome is an average mass flow rate along the entire core inlet.

The capability of the reduced order model to reproduce different situations from what included in the snapshots (Table 2) should be assessed. Even if the best option consists in calculating as much as possible snapshots related to the system behaviour in order to "train" the spatial basis, it is not possible to include every possible situation that may happen in the cold pool and therefore it is important to ensure acceptable results if the simulations cover situations not sampled in the calculated snapshots. To this purpose, a 20% and 40% velocity variation at the outlet of the second SG with respect to the nominal value (i.e., $\mathbf{u}_{SG2}$ = 0.136 m/s and $\mathbf{u}_{SG2}$ = 0.102 m/s, respectively) is considered with the full order model. The results are then compared with the ROM model built starting from the snapshots calculated beforehand (i.e., the Cases from 13 to 16, see Table 2).

In Figure 16, the L^2 error of the ROM model velocity with 80 spatial basis functions following a 20% and 40% velocity variation at the outlet of the second SG with respect to the nominal value is shown. Even if the error is around 10% at the end of the transient, the results should be read considering that these situations are not included in the snapshots set. In this case, there is no guarantee that the reduced order model can reproduce the correct behaviour. On the other hand, the ROM-based component of the coolant pool turns out to give physical results without mathematical or numerical issues. This is mainly due to the fact that in this work the CRT approach has been selected rather than SRS (see Section 3), building the reduced order model upon a robust physical model.

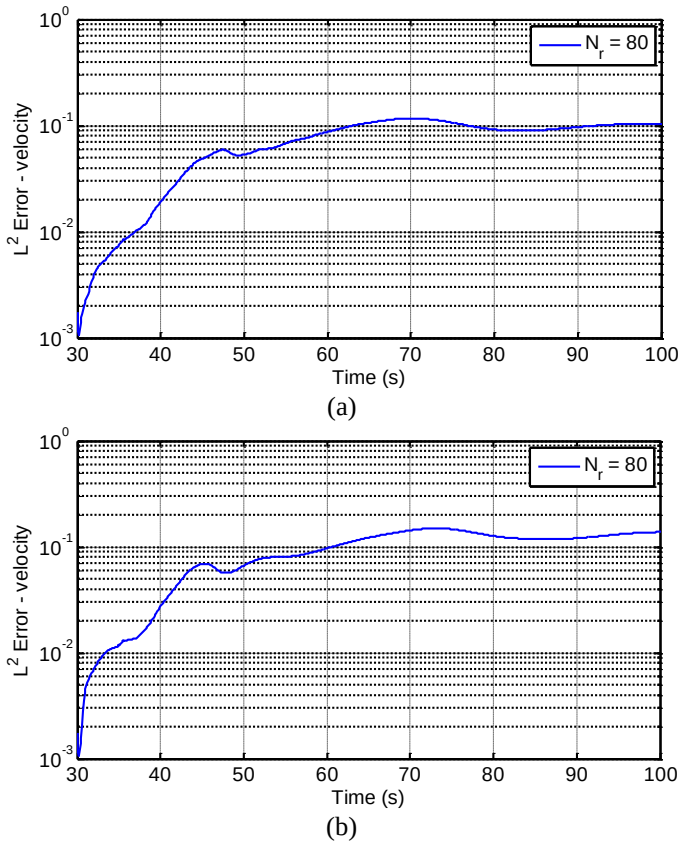

Figure 16. L^2 error of the reconstructed velocity from ROM model with N_r=80 following a variation of (a) 20% - u_{SG2}=0.136 m/s; (b) 40% - u_{SG2}=0.102 m/s with respect to the nominal value.

In addition, the assessment is performed also considering the output variable, i.e., the mass flow rate in the central FA, for the FOM model, the ROM-based component and the 0D-based component. A good agreement between the FOM model and the ROM-based component is obtained in case of 20% variation (Figure 17), whereas in the other case (Figure 18) a bigger discrepancy is found. This can be explained considering the velocity profile at the core inlet for the FOM and the ROM models (Figure 19). In particular, there is a shift in the profile between the two models, magnified by the fact that the mass flow rate behaviour in the central FA is considered. However, the result can be considered acceptable since the 0D model shows a bigger discrepancy than the ROM-based component with respect to the high fidelity model.

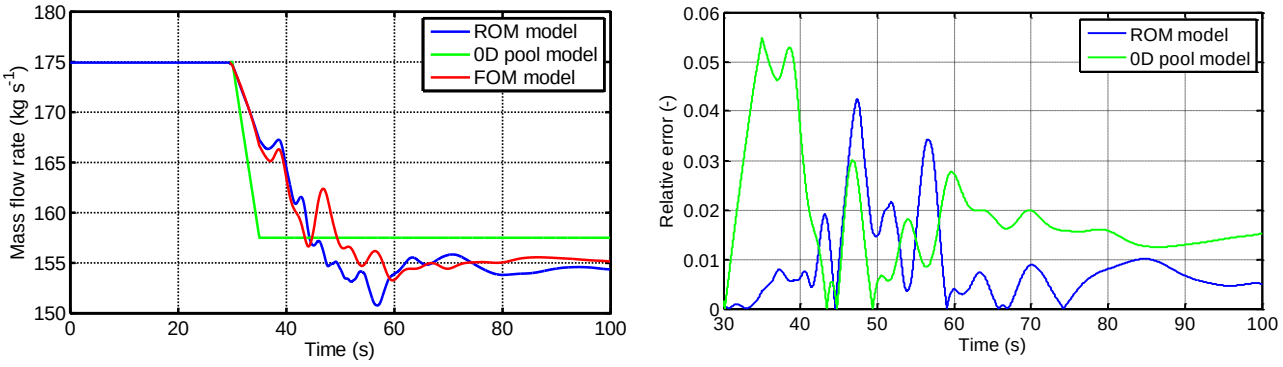

Figure 17. (a) Evolution of the mass flow rate in the central FA following a velocity variation of (a) 20% - u_{SG2}=0.136 m/s with respect to the nominal value. ROM (blue line), 0D (green line) and FOM (red line) model results; (b) relative error of ROM and 0D model with respect to FOM model.

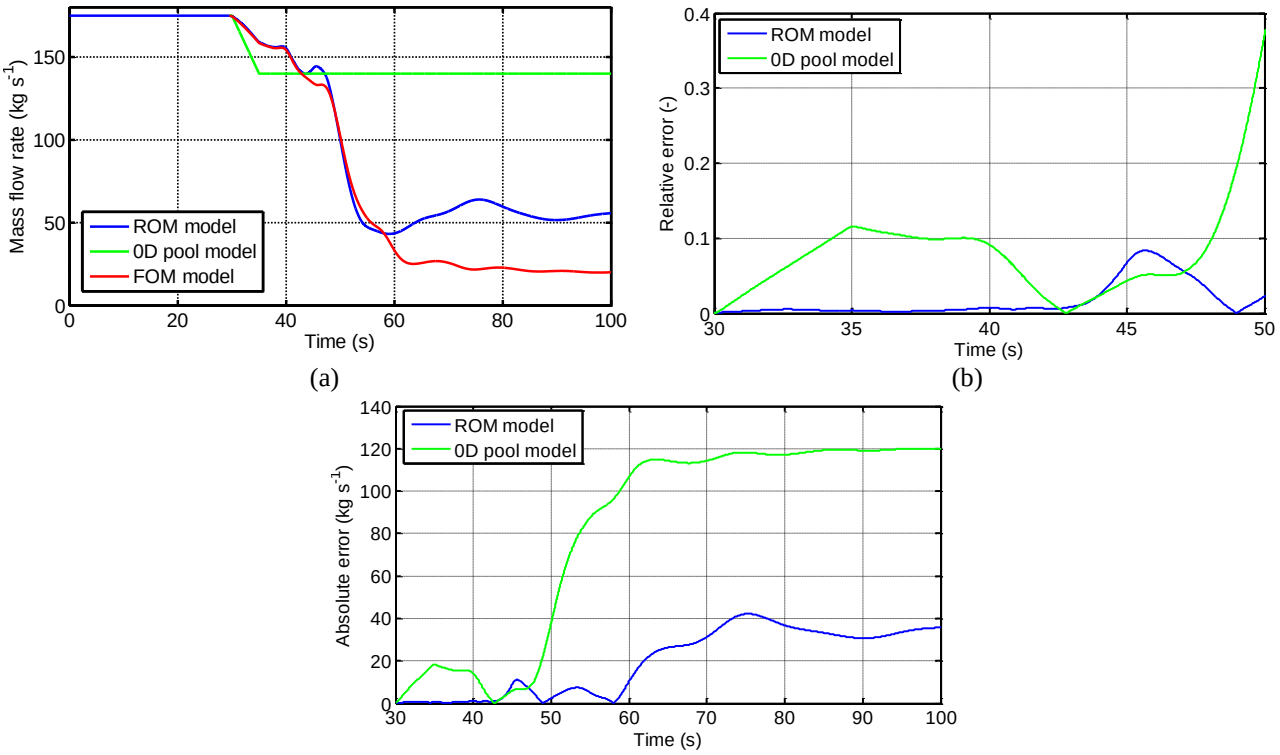

Figure 18. (a) Evolution of the mass flow rate in the central FA following a velocity variation of (a) 40% - u_{SG2}=0.102 m/s with respect to the nominal value. ROM (blue line), 0D (green line) and FOM (red line) model results; (b) relative error of ROM and 0D model with respect to FOM model (the time is limited to 50 s since the FOM mass flow rate approaches a very small value); (c) absolute error of ROM and 0D model with respect to FOM model.

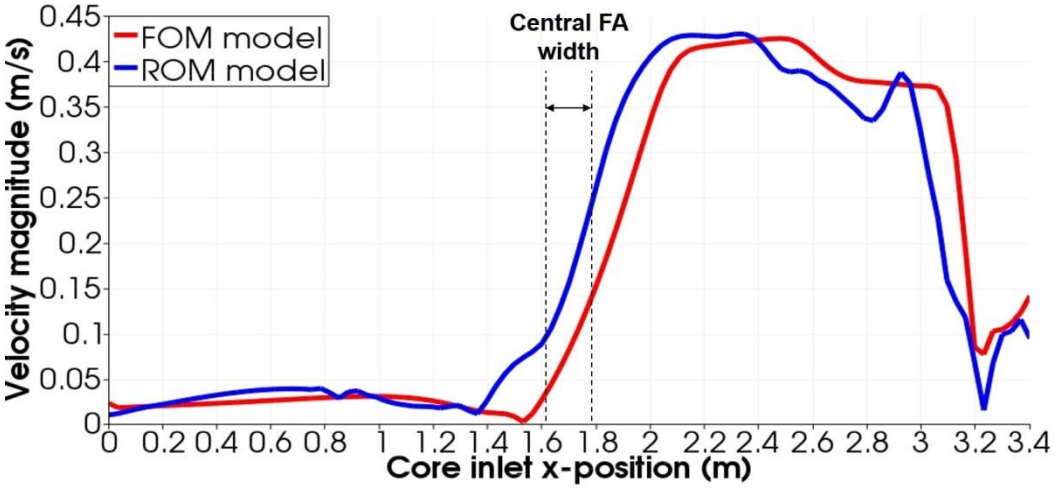

(a)

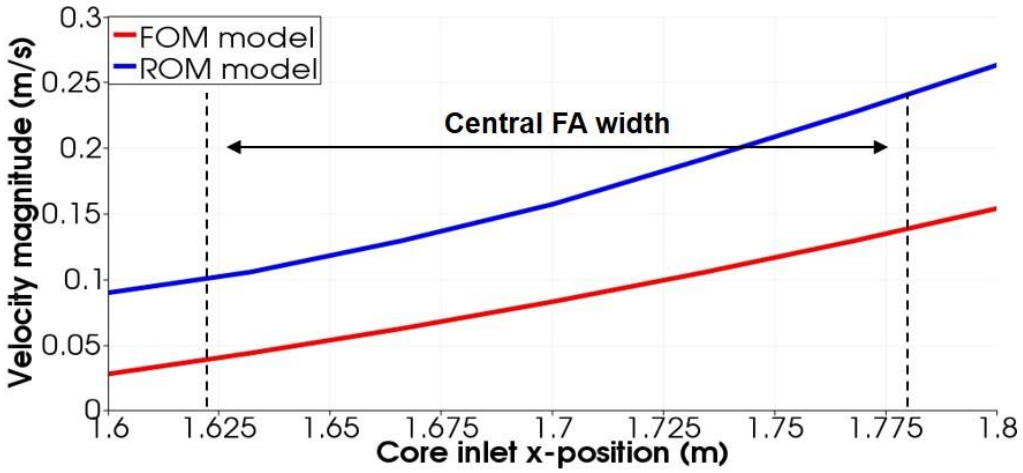

(b)

Figure 19. Velocity profile (t = 100 s) at core inlet following a velocity variation of 40% - u_{SG2}=0.102 m/s with respect to the nominal value. FOM (red line), ROM (blue line) model results.

Finally, for the full order model, a computational time of 212 cpu-hours is required for a single simulation case of 70 s (the calculations were performed on the CINECA GALILEO cluster with 16 processors). On the other hand, for the ROM model, only a computational time of 25 s (N_r=80) is needed to perform the same simulation. For the sake of completeness, for the POD generation and the ROM matrix calculation of the offline step, the procedure takes 0.3 cpu-hours and 40 cpu-hours, respectively. The previous computational time allows the control-oriented simulator to be fast-running, which is one of the requirements demanded for such modelling tool. At the same time, the simulator is improved with a more accurate physical representation of a complex phenomenon, i.e., the thermal-hydraulics in the coolant pool of ALFRED reactor.

6. Conclusion

In this paper, the development of a reduced order model for the spatial description of the coolant pool of a nuclear reactor is presented. The aim of such a modelling effort is to overcome the lumped-parameter or one-dimensional modelling usually employed in control-oriented applications. Even if these approaches are well suited for control purposes since they provide fast-running simulations and are easy to linearize, they may not be sufficient to deeply assess complex systems, in particular where spatial phenomena have a remarkable impact on dynamics. A possible solution is the use of Reduced Order Methods in order to take advantage of the high level of accuracy and the better physical description without increasing the computational burden. In particular, this paper is aimed at verifying and assessing the feasibility of employing ROM-based components in the control-oriented simulator of the ALFRED reactor plant. Among the several ROM techniques, the POD-FV-ROM has been applied since it extends the classic POD-Galerkin-ROM method to the Finite Volume approximation of the Navier-Stokes equations and makes possible the construction of a reduced order model capable to handle turbulent flows modelled through the RANS equations. In this way, it is possible to pursue the classic approach used in nuclear engineering for the turbulent flows based on the Finite Volume discretization without modifying the tools usually adopted (and validated) for this kind of problems.

Starting from this procedure, a parametric ROM-based component of the coolant pool of the ALFRED reactor has been developed, considering the possibility of varying the input variables of the model. In particular, the velocity at the SG has been considered as parametrized boundary condition since it can be a possible control variable. The variation of the velocity at the SG outlet has been shown to have an impact on the velocity profile at core inlet and, in turn, on the distribution of the mass flow rate inside the core. The simulation results show a good agreement between the ROM and the FOM models in reproducing the velocity field up to the 50% variation of the SG velocity with respect to the nominal value, the relative error of the velocity field being always lower than 5%. As a major outcome of the work, it has been shown that the ROM-based component is more accurate than 0D model without an excessive computational cost. In particular, in asymmetric transients (where the spatial information of the velocity is crucial), the ROM model correctly represents the inlet velocity profile movement from the centre to the periphery of the core. On the other hand, the 0D model is not able to capture this spatial information and the result is an average mass flow rate along the entire core inlet. Finally, the robustness of the reduced order model to reproduce different situations from what included in the snapshots has been assessed, giving acceptable results and, in any case, improving the accuracy with respect to the 0D modelling.

Finally, a spatial modelling approach of the coolant pool of a nuclear reactor has been proposed aimed at being used in a control-oriented simulator. The adopted description allows for the spatial heterogeneity of the system, in particular as concerns the velocity field, i.e., the main variable of interest. Moreover, it turns out to be employed in control-oriented applications, being accurate in both the velocity field and the output variable representation (e.g., mass flow rate) without an excessive computational cost. This modelling improvement may allow adopting innovative control strategies, whose feasibility in the nuclear field cannot be adequately studied by means of the 0D/1D approach. The ROM approach assessed in this paper is not tailored only to LFR applications but it can be employed for different reactor concepts with similar pool-type configuration, e.g., the Molten Salt Fast Reactor (http://www.samofar.eu) or the Sodium Fast Reactor (Vasile et al., 2015), and can be valuable for other fluid-dynamics applications.

As future development of this work, the inclusion of the energy equation in the POD-FV-ROM is of great interest since it allows considering also the thermal coupling in the model of the coolant pool. Moreover, some additional tests should be performed on the ROM-based components of the control-oriented simulator in order to definitively prove that no further issues arise in their employment. In particular, the coupling of different ROM-based components and the behaviour in situations quite far from the snapshot ensemble are the main topics in this direction, opening new perspectives, for example dealing with uncertainty scenarios.

Nomenclature

a_i	time coefficient, -
$\boldsymbol{a}$	time coefficient vector of the ROM model, -
$\boldsymbol{B}$	matrix of the ROM model, -
$\boldsymbol{BT}$	matrix of the ROM model, -
$\boldsymbol{C}$	matrix of the ROM model, -
$\boldsymbol{CT1}$	matrix of the ROM model, -
$\boldsymbol{CT2}$	matrix of the ROM model, -
$\boldsymbol{D}$	matrix of the ROM model, -
e	L^2 error of velocity, -
$\boldsymbol{E}$	matrix of the ROM model, -
F	face flux, $m^3\ s^{-1}$
F_r	ROM model face flux , $m^3\ s^{-1}$
k	turbulent kinetic energy, $m^2\ s^{-2}$
$\dot{m}_{FA}$	mass flow rate of the FA, $kg\ s^{-1}$
N_r	number of ROM model functions, -
N_s	number of snapshots, -
p	normalized pressure, $m^2\ s^{-2}$
p_r	ROM model normalized pressure, $m^2\ s^{-2}$
t	time, s
$\boldsymbol{u}$	velocity, $m\ s^{-1}$
$\boldsymbol{u}_n$	snapshots velocity, $m\ s^{-1}$
$\boldsymbol{u}_r$	ROM model velocity, $m\ s^{-1}$
$\boldsymbol{u}_t$	derivative of the velocity, $m\ s^{-1}$
$\boldsymbol{u}_{BC}$	Dirichlet boundary condition of velocity, $m\ s^{-1}$
$\boldsymbol{u}_{FOM}$	FOM velocity, $m\ s^{-1}$
x	horizontal coordinate, m
$\boldsymbol{x}$	Vector of spatial coordinate, m

Greek symbols

Γ	boundary function, -
μ_i	ROM model mass flow rate of the FA, $kg\ s^{-1}$
υ	kinematic viscosity, $m^2\ s^{-1}$
υ_t	turbulent viscosity, $m^2\ s^{-1}$
$\upsilon_{t,r}$	ROM model turbulent viscosity, $m^2\ s^{-1}$
$\boldsymbol{\varphi}_i$	velocity spatial modes, $m\ s^{-1}$
ϕ_i	turbulent viscosity spatial modes, $m^2\ s^{-2}$
τ	penalty factor, -
χ_i	pressure spatial modes, $m^2\ s^{-2}$
ψ_i	face flux spatial modes, $m^3\ s^{-1}$
Ω	spatial domain, m^3

Acronyms

ALFRED	Advanced Lead Fast Reactor European Demonstrator
BC	Boundary Condition
CFD	Computational Fluid Dynamics
CR	Control Rod
CRT	Computational Reduction Techniques
DAE	Differential Algebraic Equation
DNS	Direct Numerical Simulation
FA	Fuel Assembly
FE	Finite Elements
FOM	Full Order Model
FP7	7th Framework Programme
FV	Finite Volume
LEADER	Lead-cooled European Advanced DEmonstrator Reactor
LES	Large Eddy Simulation
LFR	Lead-cooled Fast Reactor
NSE	Navier-Stokes Equation
ODE	Ordinary Differential Equation
PDE	Partial Differential Equation
PID	Proportional-Integral-Derivative controllers
POD	Proper Orthogonal Decomposition
RANS	Reynolds Averaged Navier-Stokes
RB	Reduced Basis
ROM	Reduced Order Methods
SISO	Single Input Single Output
SG	Steam Generator
SR	Safety Rod
SRS	Surrogate Response Surfaces
SST	Shear Stress Transport

Acknowledgments

The work has been carried out in the framework of a collaboration between the Energy Department of Politecnico di Milano and the SISSA (International School for Advanced Studies), including a detachment of the first author at the SISSA – mathLab Department. The authors are grateful to F. Ballarin, G. Pitton, A. Sartori (SISSA, Trieste) for the fruitful conversation and suggestions about the reduced order modelling. Acknowledgment is also due to the SISSA – MathLab Department people for their contributions in many different topics.

The computing resources have been provided by the Sis14_COGESTA and Sis15_COGESTA cpu time grant allocation at CINECA supercomputing center (Bologna, Italy).

References

Alemberti, A., De Bruyn, D., Grasso, G., Mansani, L., Mattioli, D., Roelofs, F., 2013a. The European Lead Fast Reactor Strategy and the Roadmap for the Demonstrator ALFRED. In Proceedings of the International Conference on Fast Reactors and related Fuel Cycles: Safe Technologies and Sustainable Scenarios, Paris, France, March 4–7, 2013.

Alemberti, A., Frogheri, M., Mansani, L., 2013b. The Lead fast reactor Demonstrator (ALFRED) and ELFR design. In Proceedings of the International Conference on Fast Reactors and related Fuel Cycles: Safe Technologies and Sustainable Scenarios, Paris, France, March 4–7, 2013.

Alemberti, A., Smirnov, V., Smith, C. F., Takahashi, M., 2014. Overview of lead-cooled fast reactor activities. Progress in Nuclear Energy, 77, 300-307.

Ansari A. B., Esfahanian V., Torabi, F., 2016. Discharge, rest and charge simulation of lead-acid batteries using an efficient reduced order model based on proper orthogonal decomposition. Applied Energy, 173, 152–167.

Aubry, N., Holmes, P., Lumley, J., Stone, E., 1988. The dynamics of coherent structures in the wall region of a turbulent boundary layer. Journal of Fluid Mechanics, 192, 115–173.

Balajewicz, M., Dowell, E. H., 2012. Stabilization of projection-based reduced order models of the Navier–Stokes. Nonlinear Dynamics, 70, 1619–1632

Balajewicz, M., Dowell, E. H., Noack, B. R., 2013. Low-dimensional modelling of high-Reynolds-number shear flows incorporating constraints from the Navier–Stokes equation. Journal of Fluid Mechanics, 729, 285–308.

Barbagallo, A., Sipp, D., Schmid, P. J., 2009. Closed-loop control of an open cavity flow using reduced-order models. Journal of Fluid Mechanics, 641, 1–50.

Barbagallo, A., Sipp, D., Schmid, P. J., 2011. Input_output measures for model reduction and closed-loop control: application to global modes, . Journal of Fluid Mechanics, 685, 23–53.

Bergmann, M., Cordier, L., Brancher, J. P., 2005. Optimal rotary control of the cylinder wake using proper orthogonal decomposition reduced-order model. Physics of Fluids, 17, 097101.

Bergmann, M., Bruneau, C. H., Iollo, A., 2009. Enablers for robust POD models. Journal of Computational Physics, 228, 516–538.

Berkooz, G., Holmes, P., Lumley, J. L., 1993. The Proper Orthogonal Decomposition in the analysis of turbulent flows. Annual Review of Fluid Mechanics, 25, 539–575.

Bizon, K., Continillo, G., 2012. Reduced order modelling of chemical reactors with recycle by means of POD-penalty method. Computers and Chemical Engineering, 39, 22–32.

Cammi, A., Casella, F., Ricotti, M.E., Schiavo, F., 2005. Object-oriented modelling, simulation and control of IRIS nuclear power plant with Modelica. In: Proceedings of the 4th International Modelica Conference, Hamburg, Germany, March 7-8, 2005.

Carlberg, K., Farhat, C., 2008. A Compact Proper Orthogonal Decomposition Basis for Optimization-Oriented Reduced-Order Models. In Proceedings of the 12th AIAA/ISSMO Multidisciplinary Analysis and optimization Conference, Victoria, Canada, September 10–12, 2008.

Casella, F., Leva, A., 2006. Modeling of thermo-hydraulic power generation processes using Modelica. Math. Comp. Model. Dyn. Syst. 12 (1), 19 - 33.

Cazemier, W. Verstappen, R.W.C.P., Veldman, A.E.P., 1998. Proper orthogonal decomposition and low-dimensional models for driven cavity flows. Physics of Fluids, 10, 1685–1699.

Chinesta, F., Huerta, A., Rozza, G., Willcox, K., 2016. Model Order Reduction. Erwin Stein, Rene de Borst, Tom Hughes (eds), Encyclopedia of Computational Mechanics. Second Edition. John Wiley & Sons, Ltd., New York, 2016.

Cinotti, L., Smith, C.F., Sienicki, J.J., Ait Abderrahim, H., Benamati, G., Monti, S., Locatelli, G., Wider, H., Struwe, D., Orden, A., Hwang, I.S., 2007. The potential of the LFR and the ELSY project. In Proceedings of the International congress on advances in nuclear power plants, Nice, France, May 13-18, 2007.

Cinotti, L., Locatelli, G., Aït Abderrahim, H., Monti, S., Benamati, G., Tucek, K., Struwe, D., Orden, A., Corsini, G., Le Carpentier, D., 2008. The ELSY Project. In Proceedings of the International Conference on the Physics of Reactors Nuclear Power: A Sustainable Resource, Interlaken, Switzerland, September 14-19, 2008.

Cordier, L., Noack, B. R., Tissot, G., Lehnasch, G., Delville, J., Balajewicz, M., Daviller, G., Niven, R. K., 2013. Identification strategies for model-based control. Experiments in Fluids, 54:1580.

DYMOLA, 2015. Version, 2015. Dassault Systèmes, France. http://www.3ds.com/products-services/catia/products/dymola

El-Farra, N. H., Christofides, P. D., 2002. Hybrid Control of Parabolic PDE Systems. In Proceedings of the 41st IEEE Conference on Decision and Control, Las Vegas, USA, December 10–13, 2002.

Eymard R., Gallouet, T., Herbin, R., 2000. The finite volume method. In: Ph. Ciarlet, J.L. Lions (Eds.), Handbook for Numerical Analysis, North Holland, 715–1022.

Fletcher C. A. J., 1996. Computational Techniques for Fluid Dynamics, Vol. 1: Fundamental and General Techniques, Springer.

Fritzson, P., 2011. A cyber-physical modeling language and the OpenModelica environment. In Proceedings of the 7th International Wireless Communications and Mobile Computing Conference, Istanbul, Turkey, July 4–8, 2011.

Gottlieb, D., Orszag, S.A., 1977. Numerical Analysis of Spectral Methods: Theory and Applications. CBMS-NSF Regional Conference Series in Applied Mathematics. Society for Industrial and Applied Mathematics, Philadelphia.

Grasso, G., Petrovich, C., Mattioli, D., Artioli, C., Sciora, P., Gugiu, D., Bandini, G., Bubelis, E., and Mikityuk, K., 2014. The Core Design of ALFRED, a Demonstrator for the European Lead-Cooled Reactors. Nuclear Engineering and Design, 278, 287–301.

Gunzburger, M.D., 2003. Perspectives in Flow Control and Optimization in Advances in Design and Control. Society for Industrial and Applied Mathematics, Philadelphia

Hesthaven, J. S., Rozza, G., Stamm, B., 2016. Certified Reduced Basis Methods for Parametrized Partial Differential Equations. SpringerBriefs in Mathematics. Springer International Publishing.

Holmes, P., Lumley, J. L., Berkooz, G., 1996. Turbulence, Coherent Structures, Dynamical Systems and Symmetry. Cambridge Monographs on Mechanics, Cambridge University Press, Cambridge, UK.

Iliescu, T., Wang, Z., 2014. Variational multiscale proper orthogonal decomposition: Navier-stokes equations. Numerical Methods for Partial Differential Equations, 30, 641–663.

Jasak, H., 1996. Error analysis and estimation in the Finite Volume method with applications to fluid flows. PhD thesis, Imperial College, University of London.

Jasak, H., Jemcov, A., Tukovic, Z., 2007. OpenFOAM: A C++ Library for Complex Physics Simulations. In Proceedings of International Workshop on Coupled Methods in Numerical Dynamics, Dubrovnik, Croatia, September 19–21, 2007.

Kolmogorov, A. N., 1941. The local structure of turbulence in incompressible viscous fluid for very large Reynolds numbers. In Proceedings of the USSR Academy of Sciences (in Russian), 32, 16–18. Reprinted in English: Proceedings of the Royal Society A, 434, 9–13.

Kunisch, K., Volkwein, S., 2003. Galerkin Proper Orthogonal Decomposition Methods for a General Equation in Fluid Dynamics. SIAM Journal on Numerical Analysis, 40, 492–515.

Lassila, T., Rozza, G., 2010. Parametric free-form shape design with PDE models and reduced basis method. Computer Methods in Applied Mechanics and Engineering, 199(23–24), 1583–1592

Lassila, T., Manzoni, A., Quarteroni, A., Rozza, G., 2013. Model order reduction in fluid dynamics: challenges and perspectives in Reduced Order Methods for Modeling and Computational Reduction, MS&A Series, 9, 235–274, Springer Milano.

Levine, W. S., 2011. The Control Handbook. IEEE Press.

Lorenzi, S., 2015. Improvement of the Control-oriented Modelling of the Gen-IV Lead-cooled Fast Reactor: Development of Reduced Order Methods. PhD thesis, Politecnico di Milano.

Lorenzi, S., Cammi, A., Luzzi, L., Ponciroli, R., 2015. A control-oriented modeling approach to spatial neutronics simulation of a Lead-cooled Fast Reactor. Journal of Nuclear Engineering and Radiation Science, 1, 031007, 1–10.

Lorenzi, S., Cammi, A., Luzzi, L., Rozza, G., 2016. POD-Galerkin Method for Finite Volume Approximation of Navier-Stokes and RANS equations. Computer Methods in Applied Mechanics and Engineering, 311, 151-179.

Lumley, J. L., 1967. The structure of inhomogeneous turbulent flows. In Atmospheric Turbulence and RadioWave Propagation, 166–178.

Manzoni, A., Quarteroni, A., Rozza, G., 2012. Computational Reduction for Parametrized PDEs: Strategies and Applications, Milan Journal of Mathematics, 80(2), 283–309.

Menter, F. R. 1994. Two-Equation Eddy-Viscosity Turbulence Models for Engineering Applications. American Institute of Aeronautics and Astronautics Journal, 32(8), 1598–1605.

Menter, F. R., Kuntz, M., Langtry, R., 2003. Ten Years of Industrial Experience with the SST Turbulence Model. Turbulence, Heat and Mass Transfer, 4, 2003, 625–632.

Ogata, K., 2009. Modern Control Engineering. Prentice Hall.

Oliveira, I., Patera, A., 2007. Reduced-basis techniques for rapid reliable optimization of systems described by affinely parametrized coercive elliptic partial differential equations. Optimization and Engineering, 8(1), 43–65.

OpenFOAM, 2014. Version 2.3, www.openfoam.org.

Östh, J., Noack, B. R., Krajnovi¢, S., Barros, D. Borée, J., 2014. On the need for a nonlinear subscale turbulence term in POD models as exemplified for a high-Reynolds-number flow over an Ahmed body. Journal of Fluid Mechanics, 747, 515–544.

Ponciroli, R., Bigoni, A., Cammi, A., Lorenzi, S., Luzzi, L., 2014a. Object-oriented modelling and simulation for the ALFRED dynamics. Progress in Nuclear Energy, 71, 15–29.

Ponciroli, R., Cammi, A., Lorenzi, S., Luzzi, L., 2014b. A preliminary approach to the ALFRED reactor control strategy. Progress in Nuclear Energy, 73, 113–128.

Ponciroli, R., Cammi, A., Della Bona, A., Lorenzi, S., Luzzi, L., 2015a. Development of the ALFRED reactor full power mode control system. Progress in Nuclear Energy, 85, 428–440.

Ponciroli, R., Cammi, A., Lorenzi, S., Luzzi, L., 2015b. Control approach to the load frequency regulation of a Generation IV Lead-cooled Fast Reactor. Energy Conversion and Management, 103, 43–56.

Ponciroli, R., Cammi, A., Lorenzi, S., Luzzi, L. 2016. Petri-net based modelling approach for ALFRED reactor operation and control system design. Progress in Nuclear Energy, 87, 54–66.

Pope, S. B., 2000. Turbulent Flows. Cambridge University Press.

Protas, B., Noack, B. R., Östh, J., 2015. Optimal nonlinear eddy viscosity in Galerkin models of turbulent flows. Journal of Fluid Mechanics, 766, 337–367.

Quarteroni, A., Rozza, G., Manzoni, A., 2011. Certified reduced basis approximation for parametrized partial differential equations and applications. Journal of Mathematics in Industry, 1:3.

Quarteroni, A., Manzoni, A., Negri, F., 2016. Reduced Basis Methods for Partial Differential Equations. An Introduction. Springer International Publishing, Switzerland.

Richardson, L. F., 1922. Weather Prediction by Numerical Process. Cambridge University Press.

Rozza, G., Huynh, D. B. T., Patera, A. T., 2008. Reduced Basis Approximation and a Posteriori Error Estimation for Affinely Parametrized Elliptic Coercive Partial Differential Equations, Archives of Computational Methods in Engineering, 15, 229–275.

Rozza, G., Huynh, D. B. T., Nguyen, N. C., Patera, A. T., 2009. Real-time reliable simulation of heat transfer phenomena. In Proceedings of the HT2009 ASME Summer Heat Transfer Conference, San Francisco, California, USA, July 19–23, 2009.

San, O., Iliescu, T., 2013. Proper Orthogonal Decomposition Closure Models For Fluid Flows: Burgers Equation. International Journal Of Numerical Analysis And Modeling, Series B Computing and Information, 1, 1–18.

Sirisup, S., Karniadakis, G.E., 2005. Stability and accuracy of periodic flow solutions obtained by a POD-penalty method. Physica D, 202, 218–237.

Sirovich, L., 1987. Turbulence and the dynamics of coherent structures, Part I–III. Quarterly of Applied Mathematics, 45, 561–590.

Tenchine, D., 2010. Some thermal hydraulic challenges in sodium cooled fast reactors. Nuclear Engineering and Design, 240, 1195-1217.

The Modelica Association, 2014. Modelica 3.2.2 Language Specification. Available online at: http://www.modelica.org/

Tuček, K., Hermsmeyer, S., Ammirabile, L., Blanc, D., Wattelle, E., Burgazzi, L., Frogheri, M., Mansani, L., Ehster-Vignoud, S., Carluec, B., Aoust, T., Niculae, C., Elter, Z., Toth, I., 2016. Identification and categorisation of safety issues for ESNII reactor concepts. Part I: Common phenomena related to materials. Annals of Nuclear Energy, 87, 411-425.

Vasile A., Wahide C., Latge Ch., Chauvin N., Baeten P., Schyns M., Frogheri M., Mansani L., Stainsby R., Mikityuk K., Forni M., Hozer Z., 2015. The European Project ESNII Plus. In Proceedings of the International Congress on Advances in Nuclear Power Plants, Nice, France, May 3–6, 2015.

Versteeg, H. K., Malalasekera, W., 2007. An Introduction to Computational Fluid Dynamics, the Finite Volume Method. Pearson Education Limited.

Wang, Z., Akhtar, I., Borggaard, J., Iliescu, T., 2011. Two-level discretizations of nonlinear closure models for proper orthogonal decomposition. Journal of Computational Physics, 230, 126–146.

Wang, Z., Akhtar, I., Borggaard, J., Iliescu, T., 2012. Proper orthogonal decomposition closure models for turbulent flows: a numerical comparison. Computer Methods in Applied Mechanics and Engineering, 237–240, 10–26.

Weller, H. G., Tabor, G., Jasak, H., Fureby, C., 1998. A tensorial approach to computational continuum mechanics using object-oriented techniques. Computer in Physics, 12, 620–631.

Weller, J., Lombardi, E., Bergmann, M., Iollo, A., 2010. Numerical methods for low-order modeling of fluid flows based on POD. International Journal for Numerical Methods in Fluids, 63(2), 249–268.